

N94-16080

HETEROGENEITY AND SCALING LAND-ATMOSPHERIC WATER
AND ENERGY FLUXES IN CLIMATE SYSTEMS

Eric F. Wood

Water Resources Program
Princeton University
Princeton, NJ
08544

Presented at the IHP/IAHS George Kovacs Colloquium
on
Space and Time Variability and Interdependencies
in Various Hydrological Processes.

July 3 - 4, 1992

UNESCO, Paris

Abstract.

The effects of small-scale heterogeneity in land surface characteristics on the large-scale fluxes of water and energy in the land-atmosphere system has become a central focus of many of the climatology research experiments. The acquisition of high resolution land surface data through remote sensing and intensive land-climatology field experiments (like HAPEX and FIFE) has provided data to investigate the interactions between microscale land-atmosphere interactions and macroscale models. One essential research question is how to account for the small scale heterogeneities and whether 'effective' parameters can be used in the macroscale models. To address this question of scaling, three modeling experiments were performed and are reviewed in the paper. The first is concerned with the aggregation of parameters and inputs for a terrestrial water and energy balance model. The second experiment analyzed the scaling behaviour of hydrologic responses during rain events and between rain events. The third experiment compared the hydrologic responses from distributed models with a lumped model that uses spatially constant inputs and parameters. The results show that the patterns of small scale variations can be represented statistically if the scale is larger than a representative elementary area scale, which appears to be about 2 - 3 times the correlation length of the process. For natural catchments this appears to be about 1 - 2 sq km. The results concerning distributed versus lumped representations are more complicated. For conditions when the processes are non-linear, then lumping results in biases; otherwise a one-dimensional model based on 'equivalent' parameters provides quite good results. Further research is needed to fully understand these conditions.

Introduction.

The complex heterogeneity of the land surface through soils, vegetation and topography, all of which have different length scales, and their interaction with meteorological inputs that vary with space and time, result in energy and water fluxes whose scaling properties are unknown. Research into land-atmospheric interactions suggest a strong coupling between land surface hydrologic processes and climate (Charney et al., 1977; Walker and Rowntree, 1977; Shukla and Mintz, 1982; and Sud et al., 1990.) Due to this coupling, the issue of 'scale interaction' for land surface-atmospheric processes has emerged as one of the critical unresolved problems for the parameterization of climate models.

Understanding the interaction between scales has increased in importance when the apparent effects of surface heterogeneities on the transfer and water and energy fluxes are observed through remote sensing and intensive field campaigns like HAPEX and FIFE (Sellers et al., 1988). The ability to parameterize macro-scale models based on field experiments or remotely sensed data has emerged as an important research question for programs such as the Global Energy and Water Experiment (GEWEX) or the Earth Observing System (Eos). It is also important for the parameterization of the macroscale land-surface hydrology necessary in climate models, and crucial in our understanding in how to represent sub-grid variability in such macroscale models.

From a modeling perspective, it's important to establish the relationship between spatial variability in the inputs and model parameters, the scale being modeled and the proper representation of the hydrologic

processes at that scale. Figure 1 presents a schematic for modeling over a range of scales. Let us consider this figure in light of the terrestrial water balance, which for a control volume may be written as:

$$\left\langle \frac{\partial S}{\partial t} \right\rangle = \langle P \rangle - \langle E \rangle - \langle Q \rangle \quad (1)$$

where S represents the moisture in the soil column, E evaporation from the land surface into the atmosphere, P the precipitation from the atmosphere to the land surface, and Q the net runoff from the control volume. The spatial average for the control volume is noted by $\langle \cdot \rangle$.

Equation (1) is valid over all scales and only through the parameterization of individual terms does the water balance equation become a 'distributed' or 'lumped' model. By 'distributed' model, we mean a model which accounts for spatial variability in inputs, processes or parameters. This accounting can be either deterministic, in which the actual pattern of variability is represented -- examples include the European Hydrological System model (SHE) (Abbott et al., 1986a,b) and the 3-D finite element models of Binley et al. (1989) or Paniconi and Wood (1992); or statistical, in which the patterns of variability are represented statistically -- examples being models like TOPMODEL (Beven and Kirkby, 1979) and its variants (see Wood et al, 1990; Famiglietti et al., 1992a; Moore et al, 1988; and Wood et al. 1992) in which topography and soil plays an important role in the distribution of water within the catchment.

By a 'lumped' model we mean a model that represents the catchment (or control volume) as being spatially homogeneous with regard to inputs and parameters. There are a wide number of hydrologic water balance models of varying complexity that don't consider spatial variability. These range from

the well-known unit hydrograph and its variants, the water balance models of Eagleson (1978), to complex atmospheric-biospheric models being proposed for GCMs (examples being, the Biosphere Atmosphere Transfer Scheme (BATS) of Dickinson (1984) and the Simple Biosphere Model (SiB) of Sellers et al. (1986).

The terrestrial water balance, including infiltration, evaporation and runoff, has been revealed to be a highly nonlinear and spatially variable process. Yet, little progress has been made in relating the observed small-scale complexity that is apparent from recent field and remote sensing experiments to models and predictions at large scales. It is this relationship that is the subject of this paper. The research being presented represents recent work in investigating the effects of spatial variability and scale on the quantification and parameterization of the terrestrial water balance. The results draw primarily from the papers of Wood et al., (1988); Wood et al., (1990); Wood and Lakshmi (1992); and Famiglietti and Wood (1992c). Important related papers are those of Wood et al., (1986); Sivapalan et al., (1987); Beven et al., (1988); Beven (1988).

Changing Scale and Water Balance Fluxes.

Large scale field experiments such as FIFE and HAPEX, and remote sensing experiments like MAC-HYDRO (see Wood et al., 1992) and MAC-EUROPE (see Lin et al., 1993), have shown the significant variability across a catchment with regards to runoff production, soil moisture levels and actual evaporation rates. The heterogeneity in hillslope forms, soil properties and vegetation combine with variability in rainfall to produce different runoff processes and responses across hillslopes, different soil moisture conditions and interstorm (dry period) moisture redistribution and evapotranspiration.

For a hillslope, it may be possible to develop a distributed model which explicitly considers variability in soil and vegetation properties. In fact, the simulations of Smith and Hebbert (1979) show that the actual patterns of soil properties may be important in simulating the runoff response from a hillslope.

At the scale of a small catchment, it may be possible to consider the variability in topography, soil and vegetation as if they came from a stationary statistical distribution (Beven, 1988, Wood et al., 1990.) Thus the distributed model would consider patterns of variability statistically. Within a physioclimatic region, we can consider that there may be a population of small catchments that is statistically similar but whose actual patterns of topography, soil and vegetation properties and therefore responses vary quite differently (Beven, 1988).

As scale increases, so does the sample of the small catchments and therefore the sample of the properties that control the water balance fluxes. This increased sampling of small catchments leads to a decrease in the difference between small catchment responses, even though the patterns of the properties are quite different across these small catchments (Beven, 1988; Wood et al., 1990). At some scale, the variance between the hydrologic responses for catchments (or areas) should reach a minimum. Wood et al. (1988) suggested that this threshold scale be referred to as the 'Elementary Representative Area' (REA) which they define as:

the critical scale at which implicit continuum assumptions can be used without explicit knowledge of the actual patterns of topographic, soil, or rainfall fields. It is sufficient to represent these fields by their statistical characterization.

Predicting the water balance at the REA scale may very well require

considering heterogeneity at smaller scales, through its statistical characterization; it should not imply the use of equivalent and average parameters. In terms of Figure 1, changing scale helps us understand the aggregation of the output from the distributed response. The concept of the REA scale helps us in clarifying the relationship between a distributed model and the lumped model, and how this relationship may vary with scale.

In this paper we report on a series of numerical experiments that investigate aggregation and scaling of land-surface hydrological processes. Famiglietti (1992) and Famiglietti et al. (1992a,b) have developed a water and energy balance model within a TOPMODEL-like structure that predicts water and energy balance fluxes for areas of heterogeneous soil, hillslopes, rainfall and net radiation characteristics. The models are summarized in Appendix A, and were developed to predict water and energy fluxes for the Intensive Field Campaigns (IFCs) of FIFE (Famiglietti and Wood, 1992a,b) and subsequent remote sensing experiments (Wood et al., 1992; Lin et al., 1992). The models have also been used to analyze the water balance fluxes for catchments of different scales, in which the small catchments were sampled from a particular topography -- in this case the topography of the FIFE area (Famiglietti and Wood, 1992b).

The experiments that will be reported here are as follows. The first is the aggregation of distributed inputs for the water balance model; specifically the representation of soil and topography, and vegetation. The second is the aggregation of the hydrologic responses in a catchment due to rainfall during a storm event and due to evaporative demands during interstorm periods. These two sets of experiments allows us to infer the nature of aggregation in parameters and processes. The third experiment will

compare the aggregated fluxes from the distributed model to the predicted fluxes from a lumped version of the model.

Changing Scale and Model Inputs.

Scaling of Topography. Appendix A provides a summary of the water and energy balance models. The models were applied to the Kings Creek catchment in the FIFE area in Kansas. The FIFE area is 15 km x 15 km, with a rolling topography with an approximate elevation range is 325 m to 460 m. Except for heavier vegetation at the bottom of stream valleys, the vegetation consists on short crops, pasture and natural grasses. The Kings Creek catchment, which is 11.7 sq km in area, is in the north-west portion of the FIFE area in the Konza Prairie preserve. Figure 3 shows the division of the catchment into subcatchments -- the number ranging from 5 to 66 depending on the scale. All subcatchments represent hydrologically consistent units in that runoff flows out of the subcatchments through one flow point, and that the surface runoff flux across the other boundaries is zero.

Equation A.2 provides the relationship between variability in topography and soil, and variability in local water table depths and soil moisture. Wood et al. (1990) have shown that the variability in topography dominates variability in soil properties for Kings Creek. The TOPMODEL theory uses the topographic-soil index to predict local water fluxes and soil moisture. Further, as discussed earlier, larger catchments can be considered to be composed of a population of smaller catchments that are statistically similar but whose actual patterns vary quite considerably. The question remains: at what catchment scale is the sample of hillslopes and small catchments sufficiently large so that their actual patterns of the soil-topographic index can be represented statistically. The average value

of the topographic index, λ , was calculated for each of the subcatchments shown in Figure 3 and plotted against subcatchment area. Each pixel is 900 sq m. The behavior of the catchment shows that at small scales there is extensive variability in hillslope forms leading to variability in λ , but at a scale of approximately 1 sq km the increased sampling of hillslopes and small catchments leads to a decrease in the difference between topographies.

Wolock (personal communication) has found similar behavior over a wider range of scales for Sleepers River, VT. Figure 4 gives his results for λ over catchments scales up to approximately 45 sq km. Again, there appears to be a significant decrease in λ at about 1 to 2 sq km.

Scaling of Vegetation. In the first experiment, scaling of the topographic index was explored due to its role in subsurface water fluxes and the redistribution of soil moisture. Vegetation type and density determine the stomatal and canopy resistances, and therefore transpiration rates in the water and energy balance models (see equations A.3 - A.5.) What can be said about the scaling behavior of satellite derived estimates for vegetation?

Wood and Lakshmi (1992) used high resolution thematic mapper (TM) satellite data to derive the normalized difference vegetation index (NDVI), latent heat and sensible heat fluxes for the August 15, 1987 overpass and to investigate their scaling properties. The scaling for the vegetation will be reviewed here. The resolution of TM is 30 m for bands 1 through 5, and 120 m for the thermal band. The scaling question investigated here is whether averaging the TM bands prior to calculating NDVI provides the same derived quantities as would be found by calculating the quantities at the TM resolution and averaging. The equivalence of the two approaches depends on

the degree of non-linearity represented by in functions that relate NDVI to TM data.

The following procedure was followed. The normalized difference vegetation index (NDVI) was calculated at the 30 m TM resolution using:

$$NDVI = \frac{(B_4 - B_3)}{(B_4 + B_3)} \quad (2)$$

where B_3 represents band 3 (0.63 - 0.69 μm) and B_4 represents band 4 (0.76 - 0.90 μm). The first often being referred to as the red and the latter the near infrared band. The NDVI image corresponding to a TM scene acquired over the FIFE area for August 15, 1987, is given in Figure 5. The TM scene was fully calibrated before the calculations were carried out.

For the aggregated scales, two procedures were followed. One was to spatially aggregate the TM bands and then use equation (2) while the second procedure is to spatially aggregate the NDVI based on the 30 m TM data. This procedure was used for aggregation levels of 300 x 300 m, 750 x 750 m and 1500 x 1500 m. A resolution equivalent to AVHRR would lie between the last two cases. Figure 6 shows the aggregated NDVI, using the second procedure, for the aggregation level of 300 x 300 m. Comparisons between the two aggregation procedures can be best shown by a scatter plot between the aggregated 30 m-based NDVI and the NDVI derived using aggregated TM bands; these comparisons are presented in Figure 7.

One striking observation arises from comparing Figures 5 - 7. Notice that the detailed structure observable in Figure 5 is lost in Figure 6, and yet the averaged NDVI from the two aggregation schemes are essentially the same as can be seen in scatter plot of Figure 7. Figure 7 does show that a small bias exists between the two aggregation procedures but its magnitude

is rather insignificant. These results indicate that NDVI calculated from spatially averaged TM (or lower resolution AVHRR data) will be equivalent to the NDVI scaled up from the full resolution image.

Changing Scale and Derived Hydrologic Responses.

In a manner similar to the investigation of the scaling properties in topography, the scaling in infiltration and evapotranspiration were also investigated. For this study the water balance model described in Famiglietti et al. (1992a) (see Appendix A) was applied to the Kings Creek catchment of the FIFE area in Kansas. For a rainfall storm on August 4, 1987, the average runoff for the subcatchments shown in Figure 2 was calculated for two times and plotted in Figure 8 against subcatchment area measured in pixels. Notice that the runoff, Q_t is normalized by the average precipitation, \bar{P} . The same type of plot was done for selected times during an interstorm period that extended from July 18 through July 31, 1987 and is presented as Figure 9. The behavior of the catchment shows that at small scales there is extensive variability in both storm response and evaporation. This variability appears to be controlled by variability in soils and topography whose length scales are on the order of 10^2 - 10^3 m -- the typical scale of a hillslope. With increased scale, the increased sampling of hillslopes leads to a decrease in the difference between subcatchment responses.

These results are not too surprising given the linkage within the model between topography and the water balance fluxes -- namely that variations in topography play a significant role in the spatial variation of soil moisture within a catchment, setting up spatially variable initial

conditions for both runoff from rainstorms and evaporation during interstorm periods.

The results also suggest that at larger scales it would be possible to model the responses using a simplified macroscale model (given in Appendix A as equations A.6 and A.7) based on the statistical representation of the heterogeneities in topography, soils and hydrologic forcings (rainfall and potential evaporation). Predictions based on these equations are also shown in Figures 8 and 9 as the 'macroscale model'. Since the macroscale model is scale invariant, it appears as a straight line in Figures 8 and 9.

Scaling remotely sensed soil moisture. To date only a very limited number of catchments have been analyzed in the manner described here. Furthermore, they have all had moderate relief and located in regions with humid climates. For these, the REA-scale appears to be quite consistent at about 1-2 sq km for both the runoff and evaporation processes. Clearly additional catchments representing a broader range of climates and catchment sizes need to be analyzed before definitive statements concerning the REA-scale can be made.

To investigate whether these scaling results are model determined or reflective of actual hydrologic processes, a similar analysis was done using airborne radar from the MAC-HYDRO field experiment of 1990 in Mahantango Creek, PA, a USDA experimental catchment. This experiment focused on estimating soil moisture through passive microwave (L-band) radiation using the PBMR sensor with an effective spatial resolution of approximately 90 m and through an active radar sensor (AIRSAR) at C-, L- and P-band at a 6 x 12 m pixel resolution. The AIRSAR remote sensing of soil moisture for

MAC-HYDRO is described in Wood et al. (1992) and Lin et al. (1992) but basically the return from the radar is affected by surface soil moisture conditions. Confounding effects are due to topography, roughness and vegetation -- especially large forested areas which have high reflectivity.

Much of the catchment is covered with pasture and small grains and the return in L-band provides a good estimate of the surface soil moisture. The catchment was divided into 19 subcatchments that ranged in size up to 3.5 sq km. The division was done in a manner similarly to Kings Creek which is shown in Figure 2. Figure 10 plots the average return with catchment scale. Due to the small size of Mahantango Creek and the large areas of forest, the variance hasn't settled down as fast as that shown for the modeled results in FIFE. Nonetheless, the same behavior can be observed, again in the range of 1 - 2 sq km -- our proposed REA scale. The importance of the AIRSAR remote sensing results is that it provides an independent assessment based on measurements of the scaling behavior of soil moisture.

Lumped Versus Distributed Models.

Figure 1 presented a framework for considering the relationship between distributed and lumped models. In an earlier section, the behaviour of aggregated inputs and hydrologic responses lead to the concept of the representative elementary area, a scale where a statistical representation can replace actual patterns of variability. In this section we compare the output between a macroscale, distributed model and a lumped model.

The macroscale model is based on the model described as 'model-b' in Appendix A. This model has been applied to the intensive field campaign periods (IFCs) during FIFE of 1987 and can include variability in topography.

soils, net radiation and vegetation. The first two, topography and soils, leads to variations in soil moisture under the TOPMODEL framework; the latter two lead to variations in potential and actual transpiration.

A lumped representation (or what will also be referred to as a one-dimensional representation) is obtained by using spatially constant values for all of the above variables. The effect of representing the distributed model by a lumped model, or equivalently by replacing the spatially variable parameters and inputs by average values, will depend on nonlinearities in the model. Conceptually this can be seen by considering a second order Taylor's series expansion about the mean for the function $y = g[x, \theta]$ where θ are fixed parameters and x variable with mean $\mu(x)$ and variance $\sigma(x)$. A first order approximation for y is $\mu_1(y) \approx g[\mu(x), \theta]$, while a second order approximation would be

$$\mu_2(y) \approx g[\mu(x), \theta] + \frac{1}{2} \left. \frac{d^2 g}{dx^2} \right|_{\mu(x)} \sigma(x) \quad (3)$$

Differences between $\mu_1(y)$ and $\mu_2(y)$ depend on the magnitude of the second term in equation (3) -- the sensitivity term. As an illustrative example, consider the estimation of downslope subsurface flows, q_i , within TOPMODEL with and without considering variability in the local water table z_i . TOPMODEL relates q_i to z_i by $q_i = T_i \tan\beta \exp(-f z_i)$. Thus a first order approximation of the mean subsurface flow would be

$$\mu_1(q_i) = T_i \tan\beta \exp(-f \bar{z}) \quad (4)$$

while a second order approximation would be

$$\mu_2(q_i) = T_i \tan\beta \exp(-f \bar{z}) + \frac{1}{2} \{ T_i \tan\beta f \}^2 \exp(-f \bar{z}) \sigma(z_i) \quad (5)$$

If we scale $\mu_2(q_i)$ by $\mu_1(q_i)$ and use equation (A.2) to recognize that

$$\sigma(z_i) = f^2 \sigma\left(\ln \frac{\alpha T_e}{T_i \tan\beta}\right) \quad (6)$$

we obtain

$$\frac{\mu_2(q_i)}{\mu_1(q_i)} = 1 + 0.5 \sigma \left(\ln \frac{\alpha T_e}{T_i \tan \beta} \right) \quad (7)$$

Analysis of the soil-topographic index for Kings Creek yields a variance of 3.25. This results in the first order estimate for q_i of being biased low by approximately 65%. Since the subsurface flows and the local water table are related and since the local water table depth effects the surface soil moisture which subsequently determines the soil evaporation and infiltration rates, it's clear that the lumped model may very well lead to significant biases in the water balance fluxes.

For more complex models the sensitivities must be determined through simulation. For certain functions the sensitivities will change with the state of the catchment (wet or dry). For example Figure 11 gives the vegetation transpiration and soil exfiltration capacities used to model the FIFE data (Famiglietti and Wood, 1992a). Notice that at low and high soil moisture values the transpiration capacity function is essentially linear and the sensitivity would be low to soil moisture variations in these ranges. For volumetric moisture contents in the range 0.2 - 0.3, the sensitivity of the transpiration capacity function is high. As can be seen from Figure 11, sensitivity characteristics for soil exfiltration capacity would be high for soil moisture values greater than about 0.3.

To test the sensitivity due to dry soil conditions and to compare the distributed water-energy balance model to a lumped representation (one-dimensional model or a first order model), comparisons were made between the models for 5 days during the October 1987 FIFE intensive field campaign, IFC-4. This period had the driest conditions observed during the 1987 experiment. Figure 12 shows the simulations for October 5 - 9, 1987.

The models were run at a 0.5 hour time step to capture the diurnal cycle in potential evapotranspiration. Three models are compared: a fully distributed model, a macroscale model in which the spatial variability is considered statistically and a lumped one-dimensional model in which parameters and inputs are spatially constant.

The one-dimensional model predicts well the evapotranspiration during the morning and late afternoon when the atmospheric demand is low, but fails to accurately predict this flux during the middle portion of the day when soil and vegetation controls limit the actual evapotranspiration. It is during this period that the sensitivity is high and by ignoring the spatial variability in soil moisture the lumped model severely underestimates the catchment-scale evapotranspiration. During wet periods, the one-dimensional model may work quite well. This complicates the linkage between a distributed and lumped representation since the appropriateness of the simpler representation varies with the state of the system.

Results and Discussion.

The purpose of the paper is to review recent results for the scaling of water and energy fluxes from the land component of the climate system. Three sets of experiments were presented. The first was the aggregation of distributed inputs to determine their scaling properties and to determine whether a statistical representation for these parameters could be used. For topography, it appears that for catchment scales larger than about 1 - 2 sq km, a statistical representation is reasonable. The second part of this experiment studied scaling of the normalized vegetation index (NDVI) as derived from a thematic mapper (TM) overpass of the FIFE area on August 15, 1987. Variations in surface conditions due to vegetation

characteristics as well as topography and soils, leads to significant variation in the TM-derived variables, as is shown in the presented images. Nonetheless, aggregated values of the TM band data gave accurate estimates of the aggregated NDVI derived from the 30 m TM data.

The second set of experiments analyzed the hydrologic response at the catchment scale (but could easily be at a GCM grid scale) in which spatial variability in topography, soils and hydrologic inputs (rainfall, in this case) resulted in spatially variable responses. These results support the concept of the representative elementary area (REA) (Wood et al., 1988) and its usefulness in determining the scale at which the macroscale model is a valid model for the scaled process. The results of the experiments carried out here suggest that the REA concept has wide applicability for a range of climate problems and that it appears that the REA will be on the order of a few (1.5 to 3) correlation lengths of the dominant heterogeneity. At scales larger than the REA scale, there has been enough 'sampling' of the heterogeneities that the average response is well represented by a macroscale model with average parameters.

The third experiment compared evapotranspiration derived from distributed models with that derived from a lumped model. The models simulated five dry days during IFC-4 of the FIFE 1987 experiment. The non-linear behaviour of the soil and vegetation control of evapotranspiration (with respect to soil moisture) coupled the dry conditions and high mid-day potential evapotranspiration, resulted in the lumped model underestimating the evaporative fluxes. This results wouldn't be observed for very wet or very dry conditions, showing the subtle difficulties in understanding whether models can be represented by averaged parameters and inputs.

Current research suggests two competing approaches for handling sub-grid heterogeneity: (1) The first approach is based on the belief that subgrid processes have significant effect on processes at GCM-scales and that the non-linearity in subgrid scale processes prevents simple scaling. (2) The second approach is to ignore the variability in sub-grid processes, and represent these processes at larger scales through models with effective parameters. This is essentially the approach of the constant canopy biospheric models where horizontal variability is ignored. It is also the approach of using small-scale micrometeorological field studies for calibration (Sellers and Dorman, 1987; Sellers et al., 1989).

The results from the experiments presented here show a rather more complicated picture. One in which macroscale models can be constructed that account for observed variability across catchments without having to account for the actual patterns of variability. Experiments to date suggest that these macroscale models will accurately predict water and energy fluxes over a wide range of catchment conditions. With regards to one-dimensional or lumped models, they may work or they may not work depending on whether the catchment conditions (soil moisture levels, potential evapotranspiration, etc) lead to significant nonlinearities. The results presented in this paper must be balanced with the knowledge that the presented experiments were neither exhaustive nor complete. For example, the satellite experiments represented a particular condition in which the range of temperatures was reasonably small, resulting in effectively linear models that transfer radiances to fluxes. Whether such ranges are typical of natural systems is unknown until a greater number of analyses are done.

It is hoped that the experiments presented in this paper motivate

related research through a wider range of climatic data that can help resolve the basic issue concerning scaling in natural systems. What must be determined are the scaling properties for reasonably sized domains in natural systems where the range of variability (in vegetation, rainfall, radiance, topography, soils, etc) is reflective of these natural systems.

Acknowledgements.

The research presented here was supported in part by the National Aeronautics and Space Administration (NASA) through Grants NAGW-1392 and NAG-5-899; this support is gratefully acknowledged. The author also wish to thank Jay Famiglietti who helped develop the water and energy balance model for Kings Creek, Dom Thongs for helping with running the model and with the graphics and V. Lakshmi who analyzed the TM data. Finally, thanks to Keith Beven, M. Sivapalan and Jay Famiglietti whose extensive discussions over the last five years have helped form my ideas on aggregation and scaling.

References

- Abbott, M.B., J.C. Bathurst, J.A. Cunge, P.E. O'Connell, and J. Rasmussen, "An Introduction to the European Hydrological System-Systeme Hydrologique Europeen SHE, 1, History and Philosophy of a Physically-Based, Distributed Modelling System", *Journal of Hydrology*, **87**, 45-59, 1986a.
- Abbott, M.B., J.C. Bathurst, J.A. Cunge, P.E. O'Connell, and J. Rasmussen, "An Introduction to the European Hydrological System-Systeme Hydrologique Europeen SHE, 2, Structure of a Physically-Based, Distributed Modelling System", *Journal of Hydrology*, **87**, 61-77, 1986b.
- Beven, K.J., "Hillslope Runoff Processes and Flood Frequency Characteristics", in A.D. Abrahams (ed.), *Hillslope Processes*, Allen and Unwin, Boston, 1986, pp 187-202.
- Beven, K.J., "Scale Considerations", in D.S. Bowles and P.E. O'Connell (eds.), *Recent Advances in the Modeling of Hydrologic Systems*, Kluwer Academic Publishers, Dordrecht, 1988, pp 357-372.
- Beven, K. and M. J. Kirkby, "A Physically Based, Variable Contributing Area Model of Basin Hydrology", *Hydrol. Sci. Bull.*, **24(1)**, 43-69, 1979.
- Beven, K., Eric F. Wood and M. Sivapalan "On Hydrological Heterogeneity: Catchment Morphology and Catchment Response", *Journal of Hydrology*, **100**, 353-375, 1988.
- Binley, A.M., J. Elgy and K.J. Beven, "A Physically-Based Model of Heterogeneous Hillslopes", *Water Resources Research*, **25**, 1219-1226, 1989.
- Brooks, R.H. and A.T. Corey, "Hydraulic Properties of Porous Media", *Hydrology Paper No. 3*, Colorado State University, Ft. Collins, Colorado, 1964.
- Brutsaert, W., *Evaporation into the Atmosphere: Theory, History, and Applications*, D. Reidel Publishing Company, Dordrecht, 1982.

Charney, J., W. Quirk, S. Chow and J. Kornfield, "A Comparative Study of the Effects of Albedo Change on Drought in Semi-Arid Regions", *Journal of the Atmospheric Sciences*, **34**, 1366-1385, 1977.

Dickinson, R.E., "Modeling Evapotranspiration in Three Dimensional Global Climate Models" in *Climate Processes and Climate Sensitivity*, Geophysical Monograph 29, Maurice Ewing Volume 5, American Geophysical Union, Washington, D.C., 58-72, 1984.

Eagleson, P.S., "Climate, Soil and Vegetation", *Water Resources Research*, **14(5)**, 705-776, October, 1978.

Famiglietti, J.S., "Aggregation and Scaling of Spatially-Variable Hydrological Processes: Local, Catchment-Scale and Macroscale Models of Water and Energy Balance", Ph.D. Dissertation, Department of Civil Engineering and Operations Research, Princeton University, October, 1992, pp 203.

Famiglietti, J.S. and Eric F. Wood, "Aggregation and Scaling of Spatially-Variable Hydrological Processes, 2, A Catchment-Scale Model of Water and Energy Balance", submitted to *Water Resources Research*, October, 1992a.

Famiglietti, J.S. and Eric F. Wood, "Aggregation and Scaling of Spatially-Variable Hydrological Processes, 3, A Macroscale Model of Water and Energy Balance", submitted to *Water Resources Research*, October, 1992b.

Famiglietti, J.S. and Eric F. Wood, "Aggregation and Scaling of Spatially-Variable Hydrological Processes, 4, Effects of Spatial Variability and Scale on Areal-Average Evapotranspiration", submitted to *Water Resources Research*, October, 1992c.

Famiglietti, J.S., Eric F. Wood, M. Sivapalan and D.J. Thongs, "A Catchment Scale Water Balance Model for FIFE", *Journal of Geophysical Research*, November, 1992a.

- Famiglietti, J.S., P.C.D. Milly and Eric F. Wood, "Aggregation and Scaling of Spatially-Variable Hydrological Processes, 1, A Local Model of Water and Energy Balance", submitted to *Water Resources Research*, October, 1992b.
- Lin, D.-S., Eric F. Wood, M. Mancini, P. Troch and T.J. Jackson, "Comparisons of Remotely Sensed and Model Simulated Soil Moisture over a Heterogeneous Watershed", submitted to *Remote Sensing of Environment*, 1992.
- Lin, D.-S., Eric F. Wood, K. Beven and M. Mancini, "Soil Moisture Estimation During Mac-Europe'91 Using AIRSAR", 25th International Symposium on Remote Sensing and Global Environmental Change, Graz, Austria, April, 1993.
- Moore, I.D., E. M. O'Laughlin and G.J. Burch, "A Contour-Based Topographic Model for Hydrological and Ecological Applications", *Earth Surf. Processes Landforms*, **13**, 305-320, 1988.
- Paniconi, C. and Eric F. Wood, "A Detailed Model for Simulation of Catchment Scale Subsurface Hydrologic Processes", *Water Resources Research*, in press (1992).
- Sellers, P.J., and J.L.Dorman, "Testing the Simple Biosphere Model (SiB) Using Point Micrometeorological and Biophysical Data", *J. of Climate and Applied Meteorology*, **26**, 622-651, 1987.
- Sellers, P.J., Y. Mintz, Y.C. Sud and A. Dalcher, "A Simple Biosphere Model (SiB) for use within General Circulation Models", *Journal of the Atmospheric Sciences*, **43**, No. 6, 1986.
- Sellers, P.J., F.G. Hall, G. Asrar, D.E. Strebel and R.E. Murphy, "The First ISLSCP Field Experiment (FIFE)", *Bulletin of the American Meteorological Society*, **69**, 22-27, 1988.
- Sellers, P.J., W. J. Shuttleworth, J.L. Dorman, A. Dalcher and J.M. Roberts, "Calibrating the Simple Biosphere Model for Amazonian Tropical Forest using Field and Remote Sensing Data. Part I: Average Calibration with Field Data", *Journal of Applied Meteorology*, **28(8)**, 727-759, 1989.
- Shukla, J. and Y. Mintz, "The Influence of Land-Surface Evapotranspiration on Earth's Climate", *Science*, **215**, 1498-1501, 1982.

- Sivapalan, M., K.J. Beven and Eric F. Wood, "On Hydrological Similarity: 2. A Scaled Model of Storm Runoff Production", *Water Resources Research*, **23**, 2266-2278, 1987.
- Smith, R.E. and R.H.B. Hebbert, "A Monte Carlo Analysis of the Hydrologic Effects of Spatial Variability of Infiltration", *Water Resources Research*, **15**, 419-429, 1979.
- Sud, Y. C., P. Sellers, M. D. Chow, G. K. Walker and W. E. Smith "Influence of Biosphere on the Global Circulation and Hydrologic Cycle - A GCM Simulation Experiment", *Agricultural and Forestry Meteorology*, **52**, 133-188, 1990.
- Troch, P.A., M. Mancini, C. Paniconi and Eric F. Wood, "Evaluation of a Distributed Catchment Scale Water Balance Model", submitted to *Water Resources Research*, June, 1992.
- Walker, J.M. and P.R. Rowntree, "The Effect of Soil Moisture on Circulation and Rainfall in a Tropical Model", *Quart. J.R. Meteor. Soc.*, **103**, 29-46.
- Wood, Eric F., M. Sivapalan and K. Beven "Scale Effects on Infiltration and Runoff Production", in *Conjunctive Water Use*, S.M. Gorelick (ed.), IAHS Publ. **156**, 375-390, 1986.
- Wood, Eric F., K. Beven, M. Sivapalan and L. Band, "Effects of Spatial Variability and Scale with Implication to Hydrologic Modeling", *Journal of Hydrology*, **102**, 29-47, 1988.
- Wood, Eric F., M. Sivapalan and K.J. Beven, "Similarity and Scale in Catchment Storm Response", *Reviews in Geophysics*, **28(1)**, 1-18, February 1990.
- Wood, Eric F., D.P. Lettenmaier and V.G. Zartarian, "A Land Surface Hydrology Parameterization with Sub-Grid Variability for General Circulation Models", *Journal of Geophysical Research*, **97/D3**, 2717 - 2728, February 28, 1992.
- Wood, Eric F. and V. Lakshmi, "Scaling Water and Energy Fluxes in Climate Systems: Three Land-Atmospheric Modeling Experiments", *J. of Climate*, in press (1992).
- Wood, Eric F., D.-S. Lin, M. Mancini, D. Thongs, P.A. Troch, T.J. Jackson and E.T. Engman, "Intercomparisons Between Passive and Active Microwave Remote Sensing, and Hydrological Modeling for Soil Moisture", Symposium A.3, Progress in Scientific Hydrology and Water Resource Management using Remote Sensing, *Proceedings of the*

*29th Plannery Meeting of the Committee on World Space Research, (COSPAR),
Washington, D.C. August 28-September 5, 1992.*

Appendix A.: Spatially-Distributed Water and Energy Balance Models.

As shown by Beven and Kirkby (1979), variations in topography play a significant role in the spatial variation of soil moisture within a catchment, setting up spatially variable initial conditions for both runoff from rainstorms and evaporation during interstorm dry periods. Beven and Kirkby (1979) were the first to develop a saturated storm response model (TOPMODEL). This model has been further expanded to include infiltration excess runoff (see Beven, 1986; Sivapalan et al., 1987), interstorm evaporation (Famiglietti et al., 1992a) and a coupled water and energy balance model (Famiglietti et al., 1992b, Famiglietti and Wood, 1992a). These latter two models will be described below.

Grid Element Fluxes.

At the surface of each grid element, the coupled water-energy balance model (Famiglietti et al., 1992b) (which will be referred to as model-b) recognizes bare and vegetated land cover. Vegetation is further partitioned into wet and dry canopy. The soil column between the land surface and the water table is partitioned into a near surface root zone and a deeper transmission or percolation zone. At each grid element in the catchment, a land surface energy balance is used to calculate the potential evaporation for bare soil, unstressed transpiration for the dry canopy, and evaporation from the wet canopy. A canopy water balance is used to calculate the net precipitation. These variables, in conjunction with precipitation on bare soils, constitute the atmospheric forcing in the model.

The earlier water balance model of Famiglietti et al. (1992a) (which we will refer to as model-a) consisted of a single soil zone, and used computed potential evapotranspiration, E_p , as the interstorm atmospheric forcing. Land cover consisted only of bare soil even though vegetated surfaces were considered implicitly through the computation of the E_p .

The storm response portion of the models captures the spatial distribution of local characteristics, such as topography and soil type, and their role in partitioning precipitation into runoff, infiltration into the unsaturated zone and percolation from the unsaturated zone to the saturated zone. The interstorm portion of the model determines whether atmospherically demanded evapotranspiration (potential evapotranspiration, E_p) can be met by the soil-vegetation system. At locations where it can be met, actual evapotranspiration, E , is at the potential rate, at locations where it can't be met, the actual rate is at some lower, soil or vegetation controlled rate.

Infiltration and Runoff.

Soil Description. Soil type, texture, and properties are modeled using the description proposed by Brooks and Corey (1964). The five parameters utilized in this description include the saturated hydraulic conductivity, the saturation moisture content, the residual moisture content, the pore size distribution index, and the bubbling pressure, or the height of the capillary fringe above the water table. Using this soil parameterization, soil moisture and hydraulic conductivity in unsaturated soils can be described in terms of the matric head.

Local Computation of Vertical Soil Moisture Transport. The equations for vertical transport of soil moisture for model-b include infiltration into bare and vegetated soils, evaporation from bare soil, transpiration by vegetation, capillary rise from the water table, drainage from the root zone and transmission zone, and runoff from bare and vegetated soils. Each of these vertical moisture fluxes depends on the soil moisture status of the local root zone or the transmission zone, and the local soil properties. The infiltration, evapotranspiration and surface runoff fluxes also depend on local levels of atmospheric forcing. Canopy and soil water balance equations are applied at each grid element in the catchment to monitor the states of wetness in the local canopy, root zone and transmission zone.

For model-a, the infiltration and evaporation processes consider only bare soil. The atmospheric forcings of precipitation and potential evapotranspiration are provided as inputs to the model. As in model-b, it is determined by the model whether the soil-system can infiltrate the precipitation or provide the necessary water during evaporation to satisfy the atmospheric demand.

Infiltration is computed using the time compression approximation to Philip's equation to compute a local infiltration rate, g_i , under local time varying rainfall, p_i . The rate g_i is

$$g_i = \min [g_i^*(G), p_i] \quad (A.1)$$

in which G is the cumulative infiltration during the storm and g_i^* the local infiltration capacity, which is a function of initial soil wetness, G and

soil parameters. Infiltration excess direct runoff occurs when p_i exceeds g_i^* .

Water Table Dynamics. Saturated subsurface flow between catchment elements is assumed to be controlled by the spatial variability in topographic and soil properties following the TOPMODEL approach of Beven and Kirkby (1979), Beven (1986a,b) and Sivapalan et al. (1987). This approach develops a relationship between the catchment average water table depth, \bar{z} , and the local water table depth, z_i , in terms of the local topographic-soil index. This relationship is

$$z_i = \bar{z} + \frac{1}{f} \left[\lambda - \ln\left(\frac{\alpha T_e}{T_i \tan\beta}\right) \right] \quad (\text{A.2})$$

where T_i is the local soil transmissivity (saturated hydraulic conductivity divided by f), f is a parameter that describes the exponential rate of decline in soil transmissivity with depth and is assumed constant within a catchment, $\ln(T_e)$ is the areal average of $\ln(T_i)$, λ is the expected value of the topographic variable $\ln(\alpha/\tan\beta)$ and is constant for a particular catchment topography, α is the area drained through the local unit contour, and β is the local slope angle.

Drainage (baseflow) between storm events is assumed to follow an exponential function of average depth to the water table (soil wetness) and has the form $Q_s = Q_0 \exp(-f \bar{z})$ where $Q_0 = AT_e \exp(-\lambda)$, A being the catchment area. Given a recession curve prior to a storm, Troch et al. (1992) have developed a procedure for estimating \bar{z} and hence using (A.2) to provide the initial patterns of local water table depths, saturated areas and soil moisture values. The areal average water table depth is updated by

consideration of catchment-scale mass balance.

Evapotranspiration. For model-b, evaporation from the surface is based on solving the energy balance equation, $R_n = \lambda E + H + G$, which links the energy balance to the water balance through λE , the latent heat flux term. Here R_n refers to the net radiation at the land surface, H to the sensible heat flux and G the ground heat flux. A bulk transfer formulation for latent heat flux can be represented by (Brutsaert, 1982)

$$\lambda E = \frac{\rho C_p (e^*(T_1) - e_a)}{\gamma (r_a + r_{st})} \quad (A.3)$$

where ρ is the density of air, C_p is the specific heat of air at constant pressure, γ is the psychrometric constant, $e^*(T_1)$ is the saturation vapour pressure at the temperature of the surface, T_1 , and e_a is the vapour pressure at a reference level above the soil or canopy surface, r_a is an aerodynamic resistance and r_{st} is a bulk stomatal resistance. Equation (A.3) can be linearized about a suitable temperature, such as the air temperature T_a , leading to the Penman-Monteith formulation. In model-b the evaporation from the wet canopy is determined by the energy balance equations for the temperature of the wet vegetated surface. Setting the aerodynamic resistance consistent with the type of vegetation surface, $r_c = 0$, and letting T_1 represent the temperature of the wet vegetated surface yields the partitioning of R_n into λE and H . The unstressed transpiration from a canopy, E_c^* , whose density is represented by a leaf area index (LAI), is obtained from (A.3) in which r_{st} is replaced with a canopy resistance $r_c = r_{st}/LAI$. Here, r_{st} is a minimum resistance corresponding to the wet vegetated surface.

The potential evaporation for bare soil is calculated using the nonlinear energy balance equations described above with G nonzero, r_{st} equal zero, aerodynamic resistance consistent with the particular type of soil and T_1 referring to the temperature of the wet bare soil. The actual evaporation for the soil is found by applying a desorptivity based Philip-like evaporation equation like the that given in (A.1) for infiltration..

For a dry canopy the actual rate of transpiration, E_c , is related to the soil moisture through

$$\tau = \frac{\psi_s - \psi_p}{R_s + R_p} \quad (A.4)$$

where τ is the transpiration supply, ψ_s is the soil matric potential, ψ_p is the plant water potential, R_s is the hydraulic resistance of the soil and R_p is the hydraulic resistance of the plant. The actual transpiration rate is given as

$$E_c = \min[\tau, E_c^*] \quad (A.5)$$

Catchment-Scale Water and Energy Fluxes. The catchment-scale water and energy balance fluxes can be computed two ways. The first is when the models are run in a 'fully distributed' mode in which the fluxes are computed grid by grid. In this mode, the grid size is usually taken to be the resolution of the digital elevation model (DEM) for the topography and therefore the resolution at which the topographic index is computed. Thus the catchment scale water balance fluxes is just the summation over all the elements whose flux values are determined from the process equations discussed above. In this mode, patterns of inputs (like vegetation, precipitation, radiation, etc) can be included in the flux calculations.

The second approach is to employ the similarity assumption inherent in TOPMODEL; namely that points in the catchment with the same value of the soil-topographic index respond similarly hydrologically. Since soil moisture is a dominant variable for the water and energy fluxes, this assumption appears quite reasonable. In this approach, fluxes will be determined conditional on values of the soil-topographic index, $\ln(\alpha T_e / T_i \tan\beta)$. For cases where significant variation occurs (like vegetation characteristics) within an area, the conditioning can be taken one step further -- i.e. calculate the fluxes conditional on $\ln(\alpha T_e / T_i \tan\beta)$ and vegetation. This conditioning approach leads to macroscale models for infiltration and evapotranspiration, which are described below.

Macroscale model for infiltration and runoff. Using the statistical distribution of the topographic-soil index, one can determine the fraction of the catchment that will be saturated due to the local soil storage being full. These areas will generate saturation excess runoff at the rate \bar{p} , the mean rainfall rate. For that portion of the catchment where infiltration occurs, the local expected runoff rate at time t , m_q , can be calculated as the difference between the mean rainfall rate, \bar{p} , and the local expected infiltration rate, m_g . This implies that m_q and m_g are conditioned upon a topographic-soil index whose statistical distribution is central to the REA macroscale model. The difference between averaged rainfall and infiltration can be expressed as

$$m_q\{t|\ln(\alpha T_e / T_i \tan\beta)\} = \bar{p} - m_g\{t|\ln(\alpha T_e / T_i \tan\beta)\}. \quad (\text{A.6})$$

As discussed above, m_q and m_g are time varying functions whose values at any particular time are equal for points within the catchment having the same

topographic-soil index; this dependence is indicated in equation (A.6) by the |. The full development of the topographic-soil index is provided in Beven and Kirkby (1979), Beven (1986a,b), Sivapalan et al. (1987) and Wood et al. (1990). Both the local expected runoff rate and the local expected infiltration rate are (probabilistically) conditioned on the topographic-soil index, $\ln(\alpha T_e / T_i \tan \beta)$. The runoff production from the catchment is found by integrating, usually numerically, the conditional rate over the statistical distribution of topographic-soil index.

Macroscale model for evapotranspiration. In a similar way, a macroscale evaporation model is developed for interstorm periods. As stated earlier, topography plays an important role in the interstorm redistribution of soil moisture and therefore in the initial conditions for the evaporation calculations. For those portions of the catchment for which the soil column can deliver water at rate sufficient to meet the potential evapotranspiration or atmospheric demand rate, E_p , the actual rate E equals E_p ; otherwise, the rate will be at a lower soil controlled rate E_s . Within the TOPMODEL framework, locations with the same value of the topographic-soil index will respond similarly; implying a macroscale model of the following form, which is conditioned on that index.

$$m_E \{t | \ln(\alpha T_e / T_i \tan \beta)\} = \min[m_{E_s} \{t | \ln(\alpha T_e / T_i \tan \beta)\}, \bar{E}_p(t)] \quad (A.7)$$

where m_E refers to the mean evaporation rate at locations in the catchment with the same index, m_{E_s} refers to the mean soil controlled rate and \bar{E}_p to the spatially average potential or atmospheric demand rate.

List of Figures.

Figure 1: Schematic of Aggregation and Scaling in Hydrologic Modeling.

Figure 2: Natural subcatchment divisions for Kings Creek, Kansas.

Figure 3: Comparisons of λ , mean of $\ln\left(\frac{\alpha}{\tan \beta}\right)$, for the subcatchments of Kings Creek, KS shown in Figure 2. Each pixel is 0.9 sq km.

Figure 4: Comparisons of λ , mean of $\ln\left(\frac{\alpha}{\tan \beta}\right)$, for the subcatchments of Sleepers River, VT. (a) for catchments up to 1 sq km, (b) for catchments up to 5 sq km, (c) for catchments up to 45 sq km. (Wolock, personal communication).

Figure 5: Normalized vegetation index (NDVI) derived for part of the FIFE area from the August 15, 1987 overpass. Resolution is 30 m.

Figure 6: 300 x 300 m aggregated normalized vegetation index (NDVI) for part of the FIFE area for August 15, 1987. The images were derived using data from Figure 5.

Figure 7: Comparisons between NDVI derived from aggregated NDVI data of Figure 9 and derived from Equation (2) using aggregated thematic mapper (TM) data. Levels of aggregation are (a) 300 x 300 m, (b) 750 750 m, (c) 1500 x1500 m..

Figure 8: Comparison of storm runoff generated from the distributed model-a (see Appendix A) and from the macroscale water balance model (Equation A.6) for two time intervals on August 4, 1987; (a) 8:45 am, and (b) 9:30 am.

Figure 9: Comparison of interstorm evapotranspiration from the distributed model-a (see Appendix A) and from the macroscale water balance model (Equation A.7) for four times during the July 18 - 31, 1987 interstorm period.

Figure 10: Comparisons of the average radar return (L-band, HH-polarization) in digital numbers for subcatchments within Mahantango Creek, PA. Data from the July 10, 1990 AIRSAR acquisition.

Figure 11: Transpiration and soil exfiltration capacities versus volumetric soil moisture content, after Famiglietti and Wood (1992a).

Figure 12: Computed catchment-average evapotranspiration from the distributed model-b (see Appendix A), the statistically aggregated macroscale model, and a lumped, one-dimensional model with spatially constant parameters. Results are for Kings Creek, KS for October 5-9, 1987.

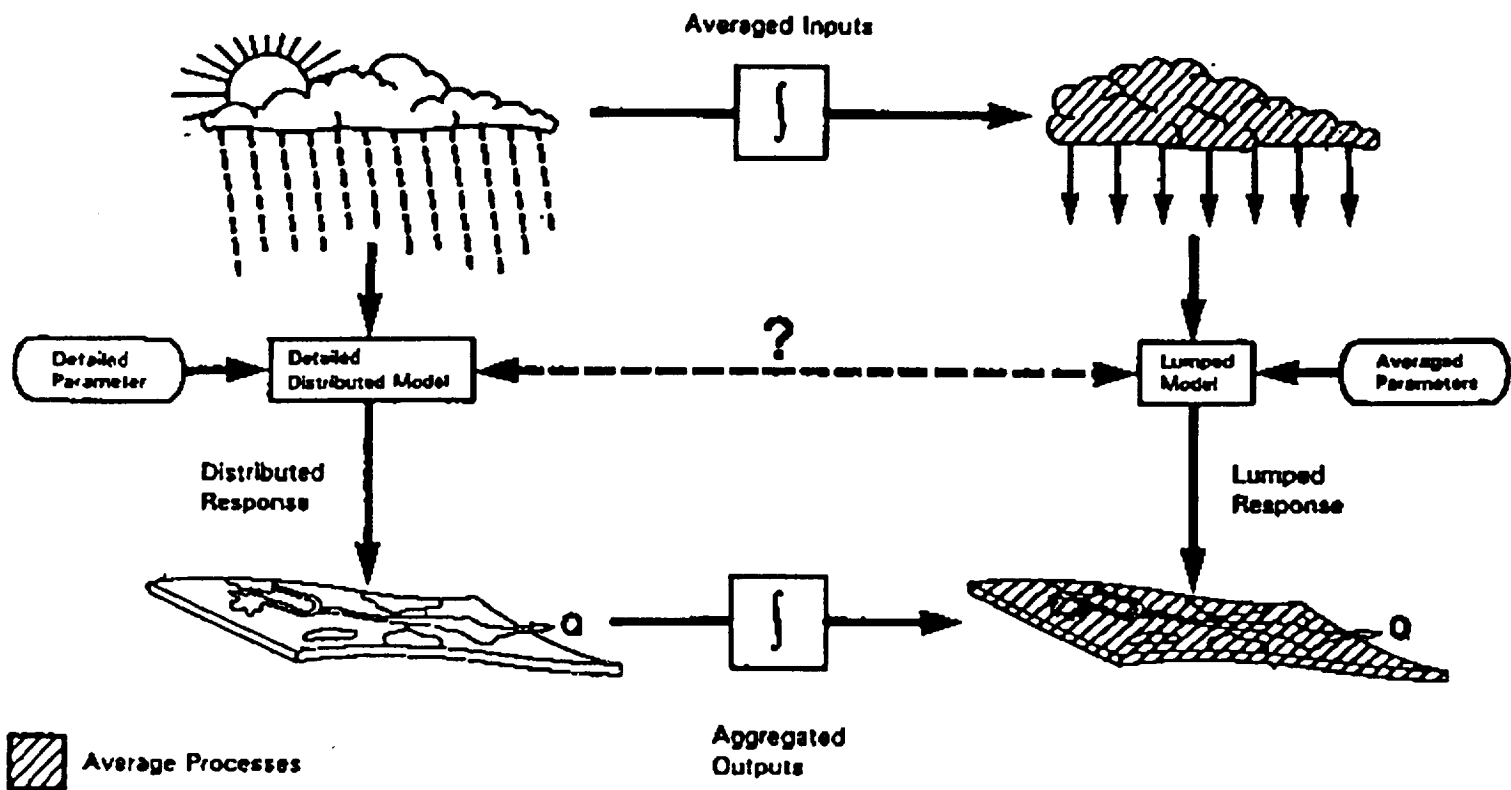


Figure 1: Schematic of Aggregation and Scaling in Hydrologic Modeling.

Ln (A/Tan(b)) / FIFE Sub-Catchment area

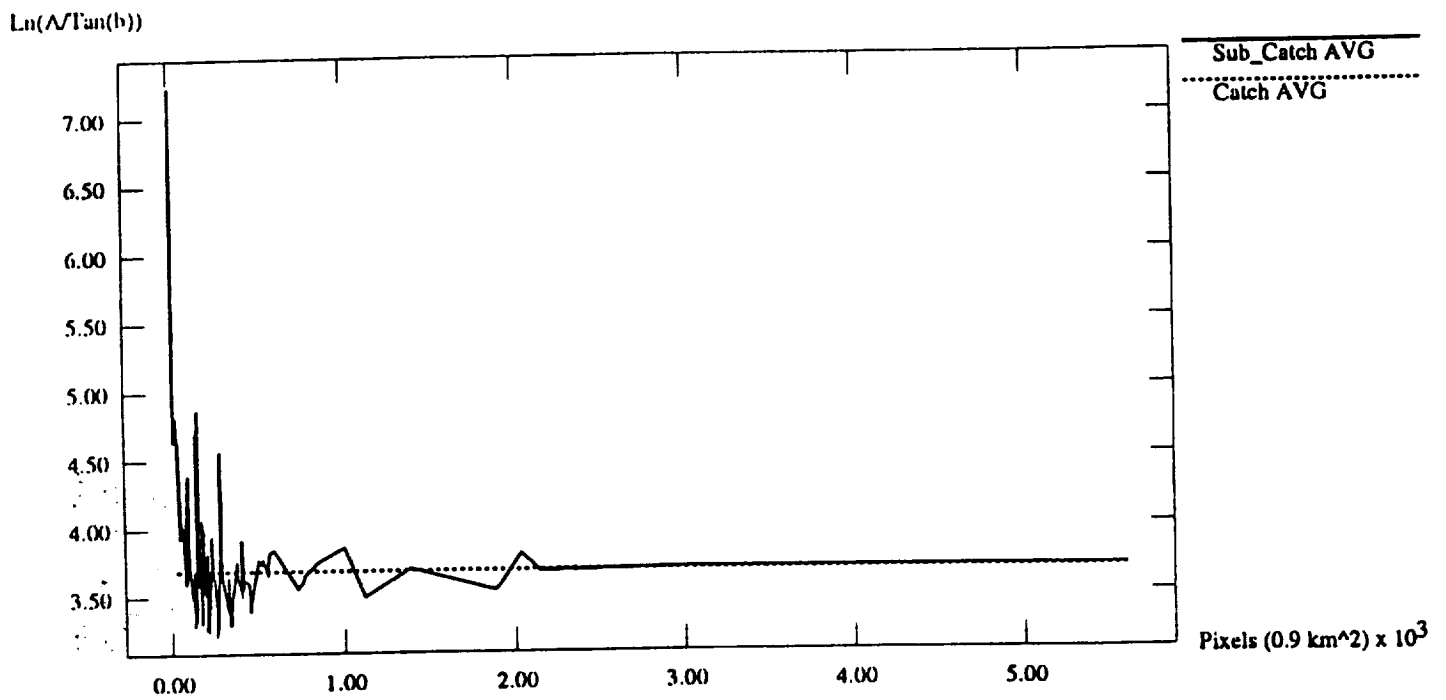


Figure 3: Comparisons of λ , mean of $\ln\left(\frac{a}{\tan \beta}\right)$, for the subcatchments of Kings Creek, KS shown in Figure 2. Each pixel is 0.9 sq km .

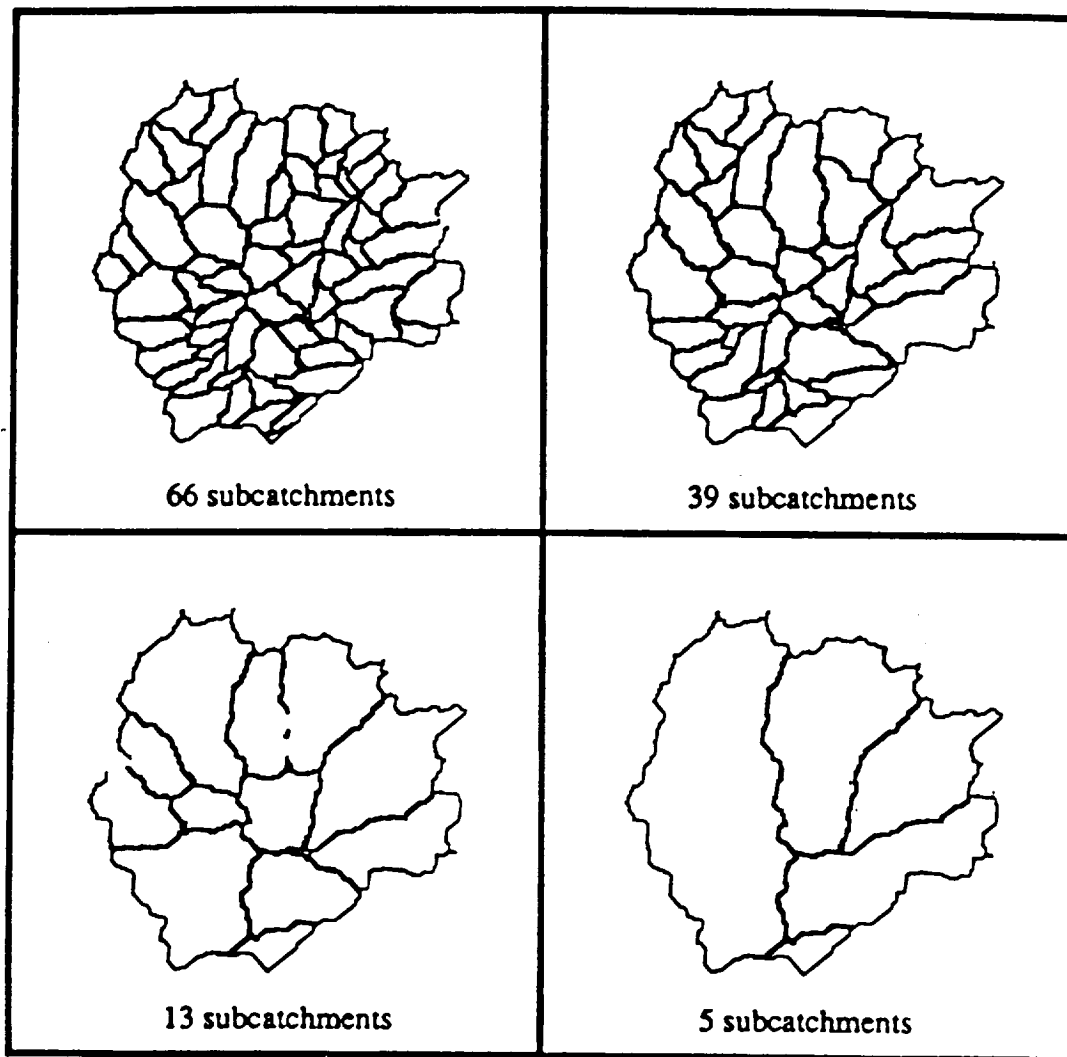


Figure 2: Natural subcatchment divisions for Kings Creek, Kansas.

Sleepers River

Mean of $\ln(a/\tan B)$ distribution

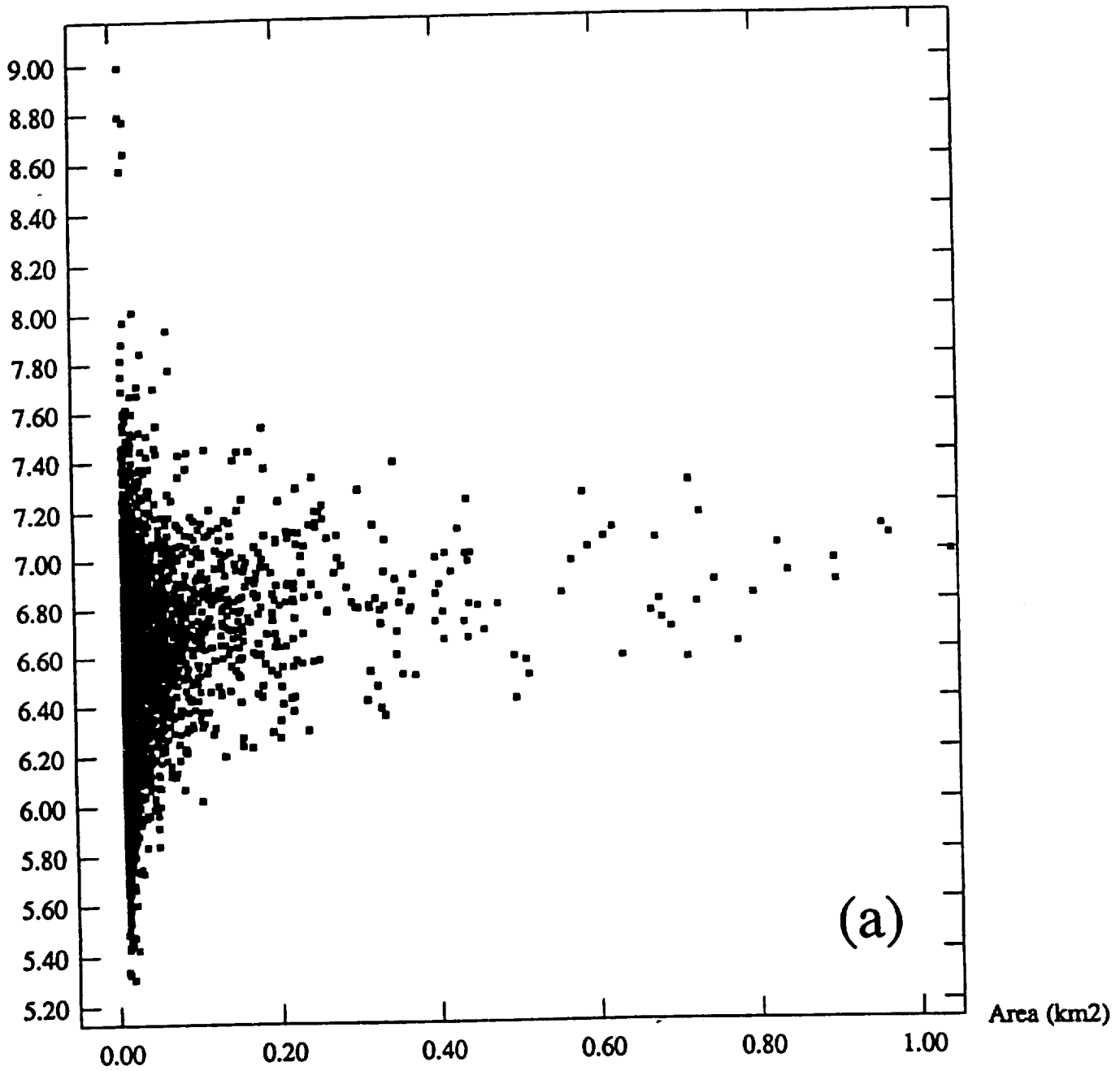


Figure 4: Comparisons of λ , mean of $\ln\left(\frac{a}{\tan \beta}\right)$, for the subcatchments of Sleepers River, VT. (a) for catchments up to 1 sq km. (Wolock, personal communication).

Sleepers River

Mean of $\ln(a/\tan\beta)$ distribution

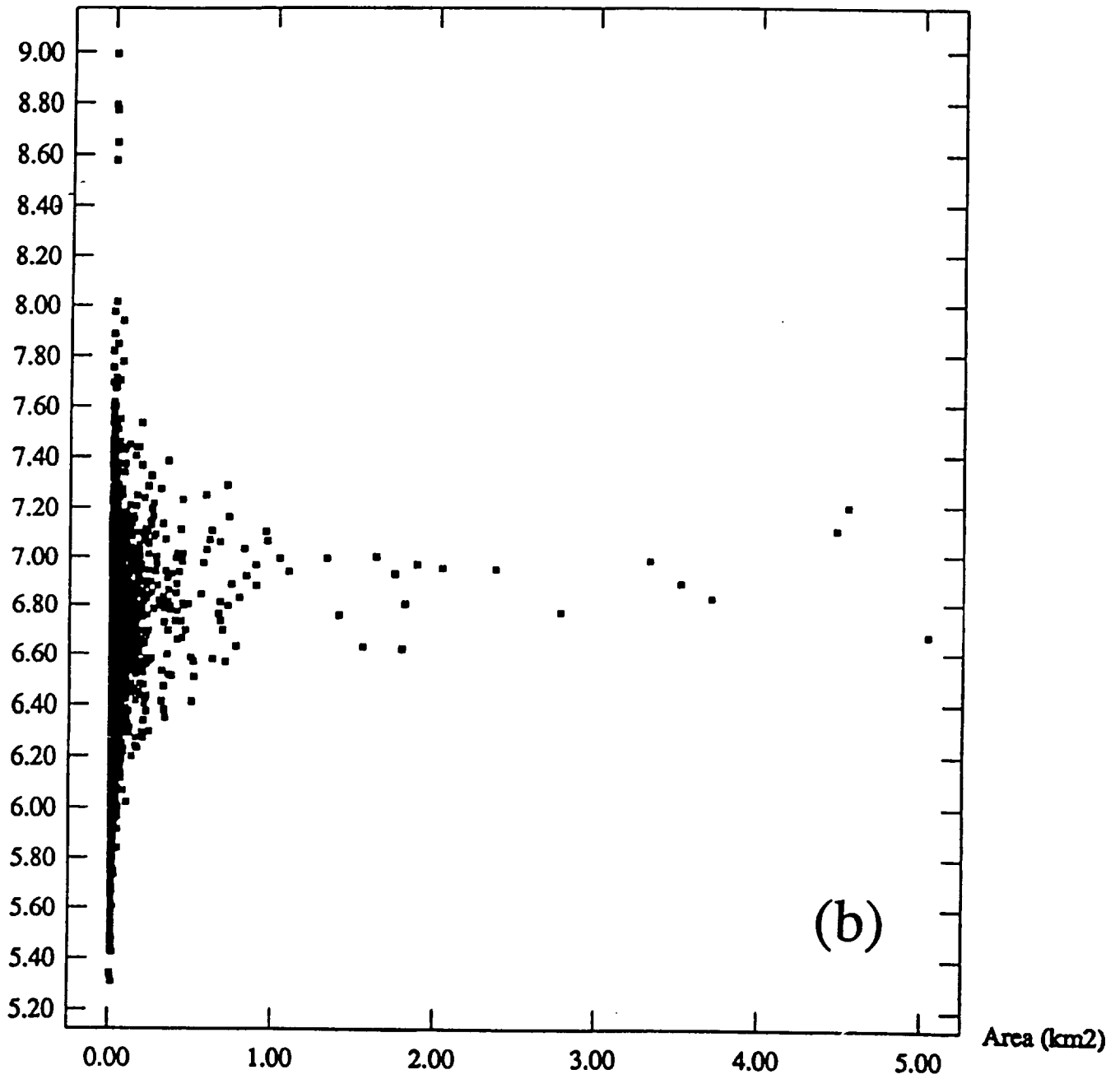


Figure 4: Comparisons of λ , mean of $\ln\left(\frac{a}{\tan\beta}\right)$, for the subcatchments of Sleepers River, VT. (b) for catchments up to 5 sq km. (Wolock, personal communication).

Sleepers River

Mean of $\ln(a/\tan B)$ distribution

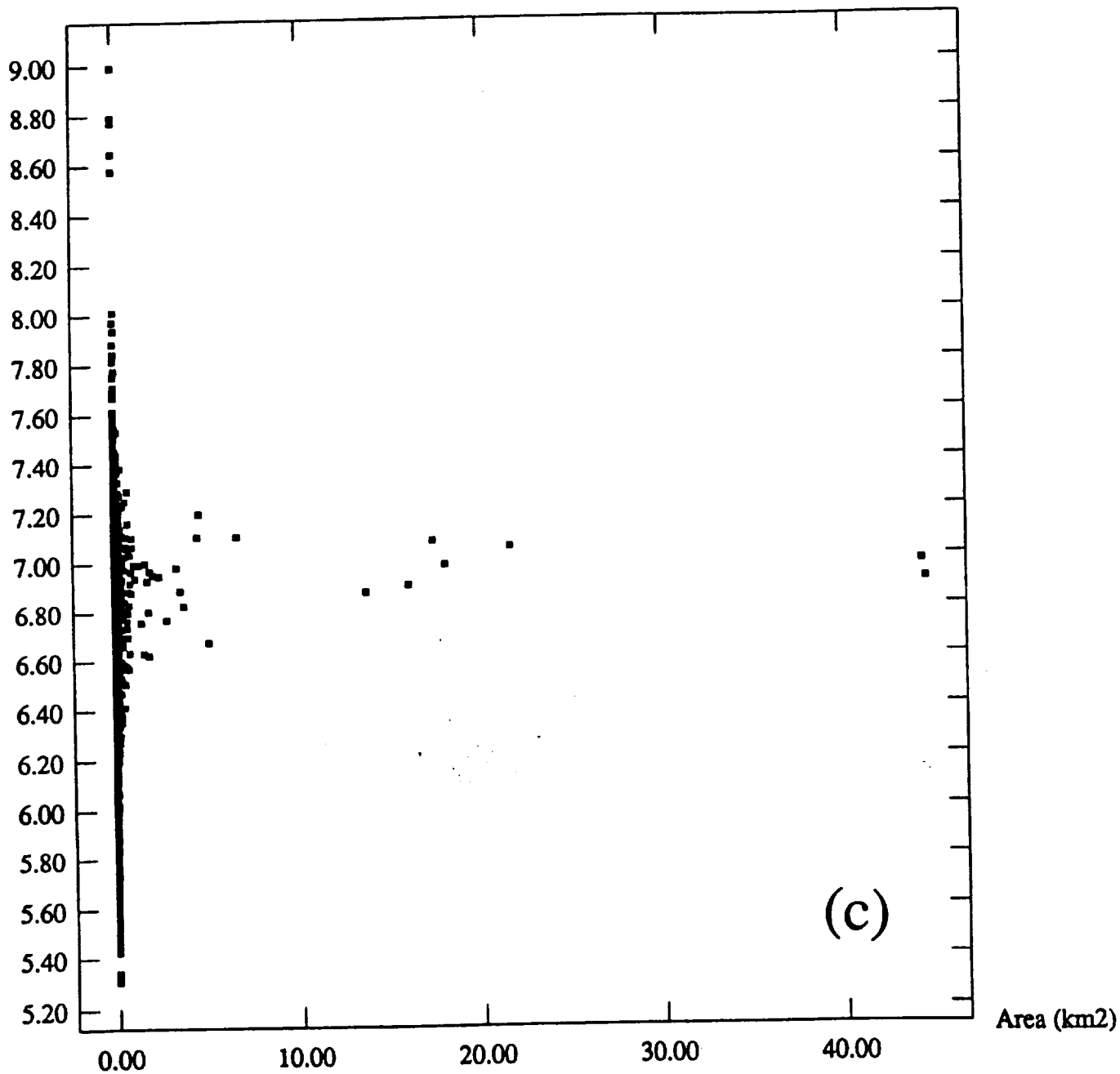


Figure 4: Comparisons of λ , mean of $\ln\left(\frac{a}{\tan \beta}\right)$, for the subcatchments of Sleepers River, VT. (c) for catchments up to 45 sq km. (Wolock, personal communication).

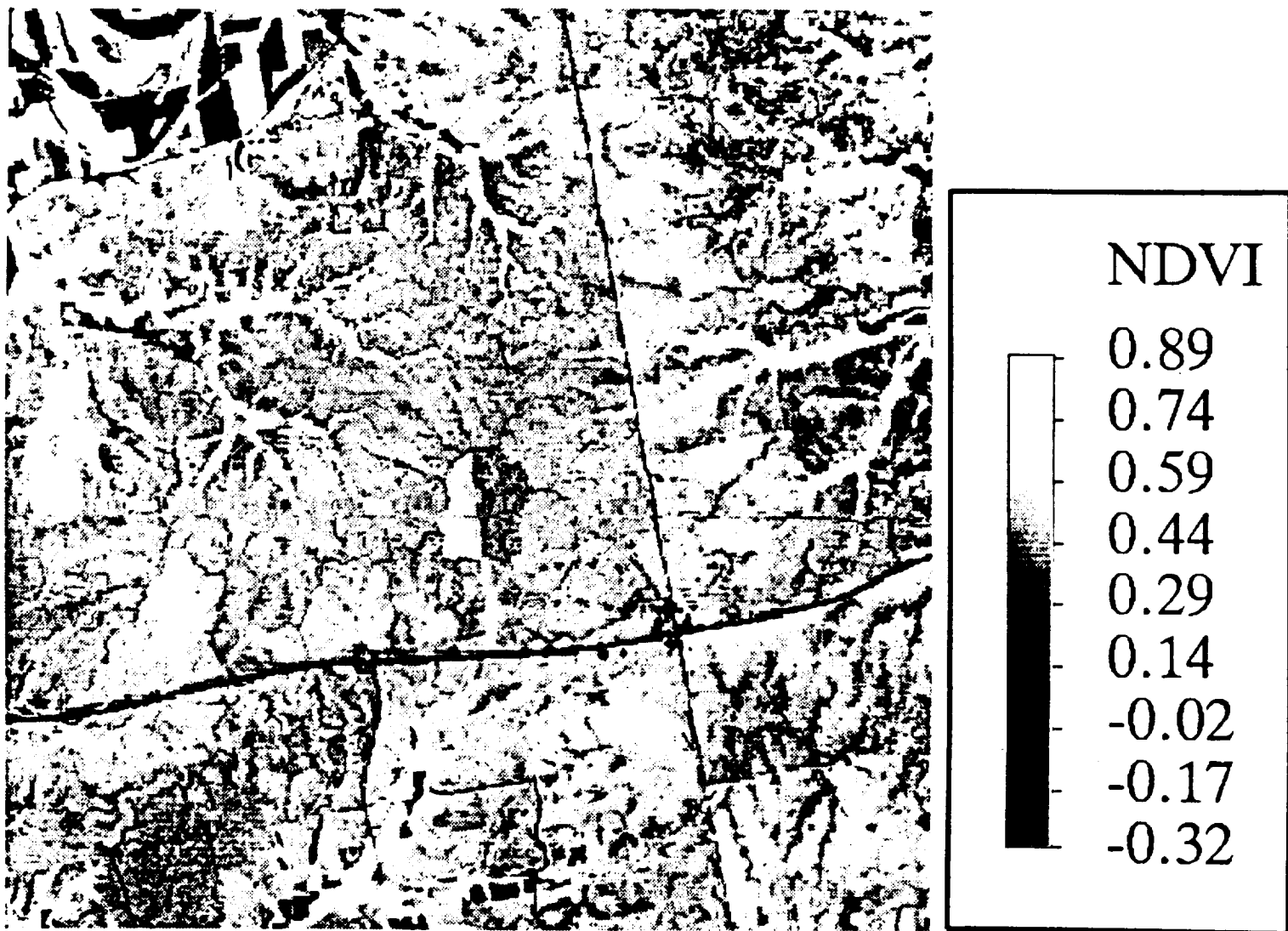


Figure 5: Normalized vegetation index (NDVI) derived for part of the FIFE area from the August 15, 1987 overpass. Resolution is 30 m.

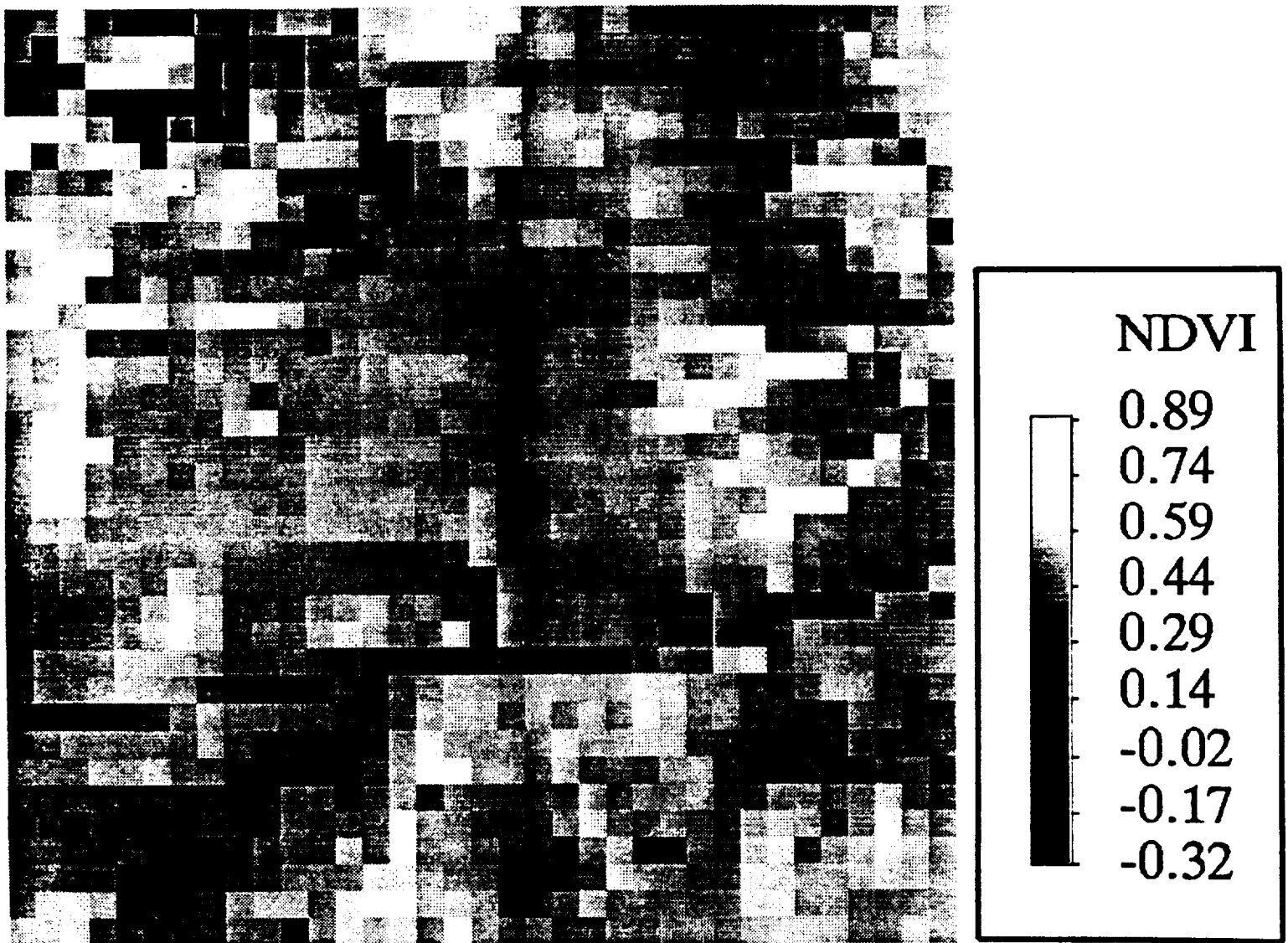


Figure 6: 300 x 300 m aggregated normalized vegetation index (NDVI) for part of the FIFE area for August 15, 1987. The images were derived using data from Figure 5.

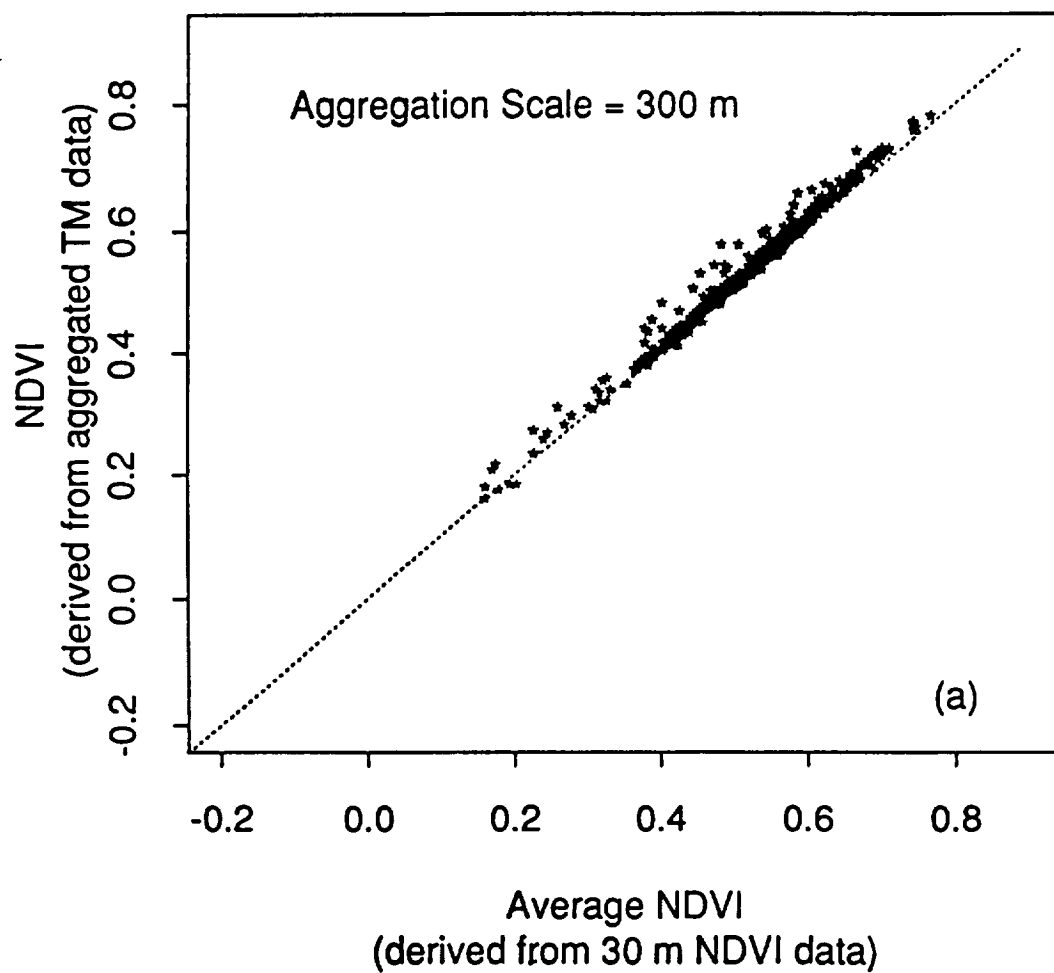


Figure 7: Comparisons between NDVI derived from aggregated NDVI data of Figure 9 and derived from Equation (2) using aggregated thematic mapper (TM) data. Levels of aggregation are (a) 300 x 300 m.

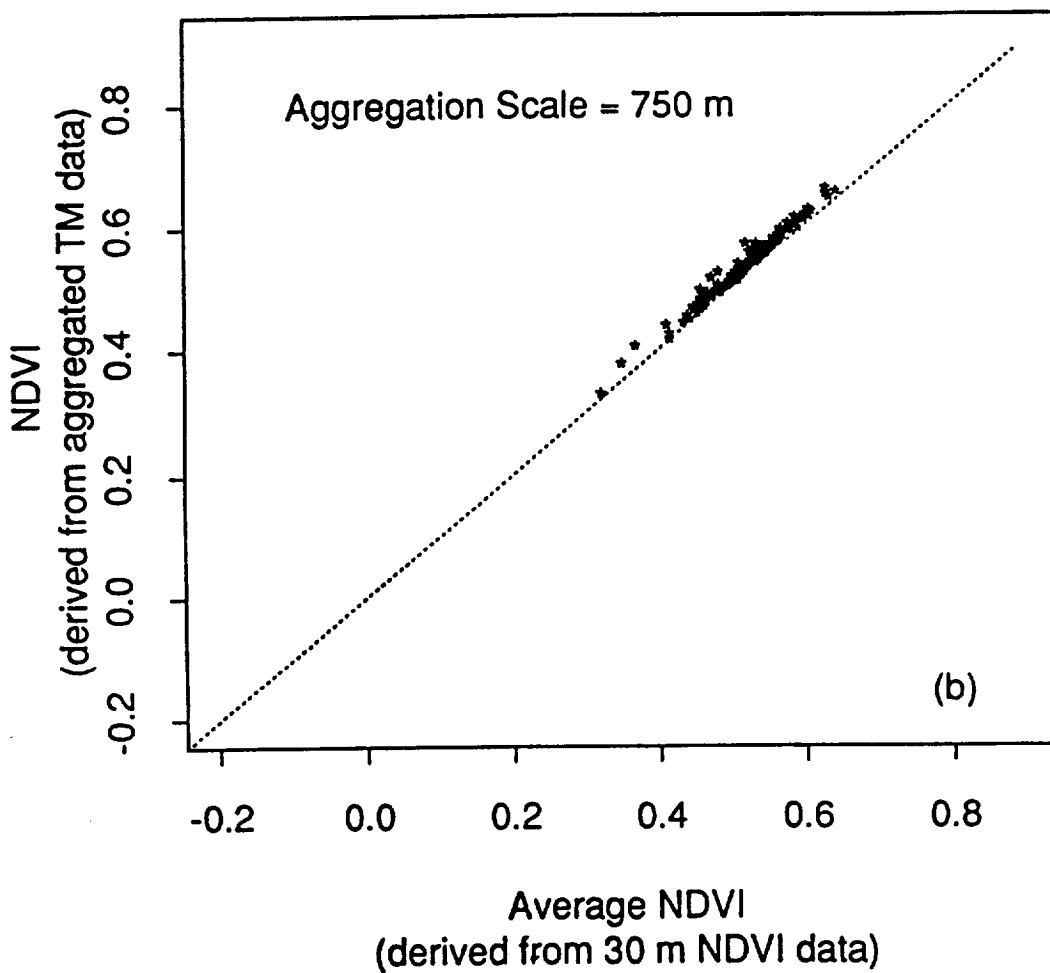


Figure 7: Comparisons between NDVI derived from aggregated NDVI data of Figure 9 and derived from Equation (2) using aggregated thematic mapper (TM) data. Levels of aggregation (b) 750 750 m.

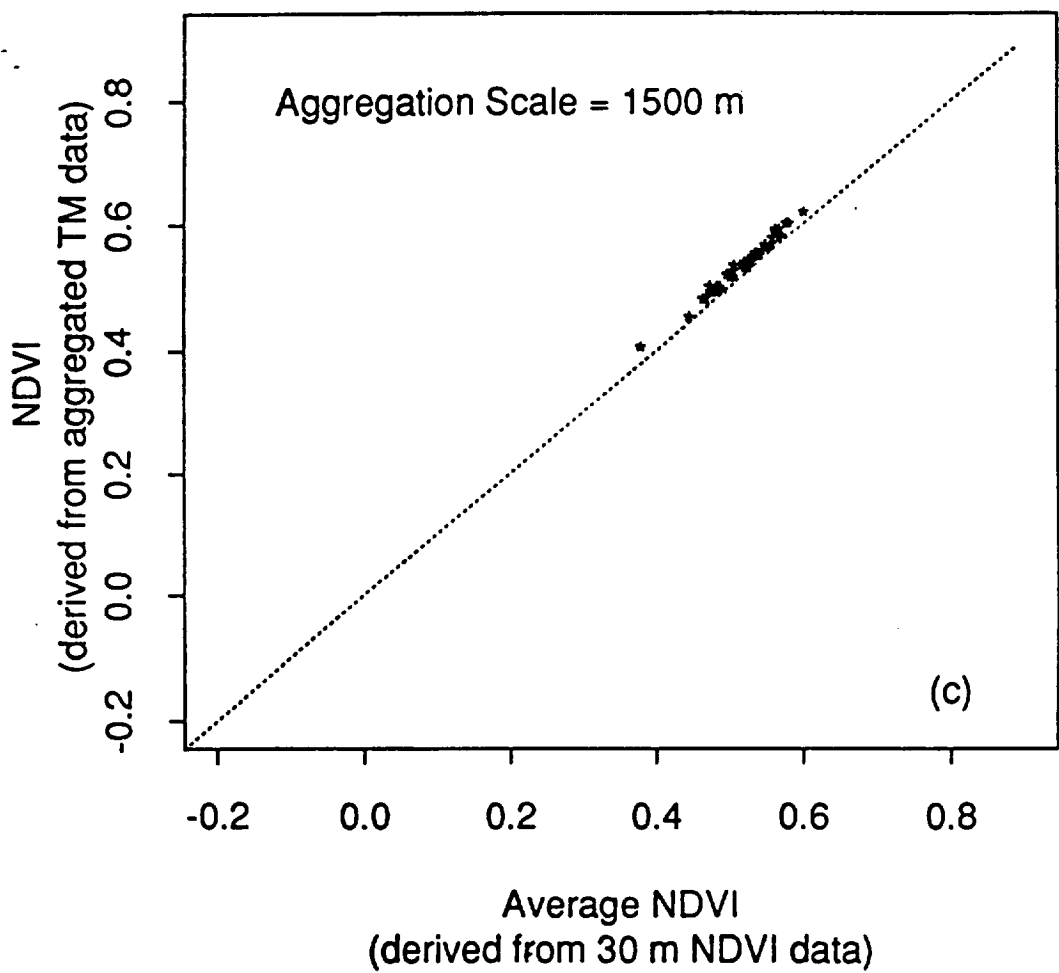


Figure 7: Comparisons between NDVI derived from aggregated NDVI data of Figure 9 and derived from Equation (2) using aggregated thematic mapper (TM) data. Levels of aggregation (c) 1500 x1500 m.

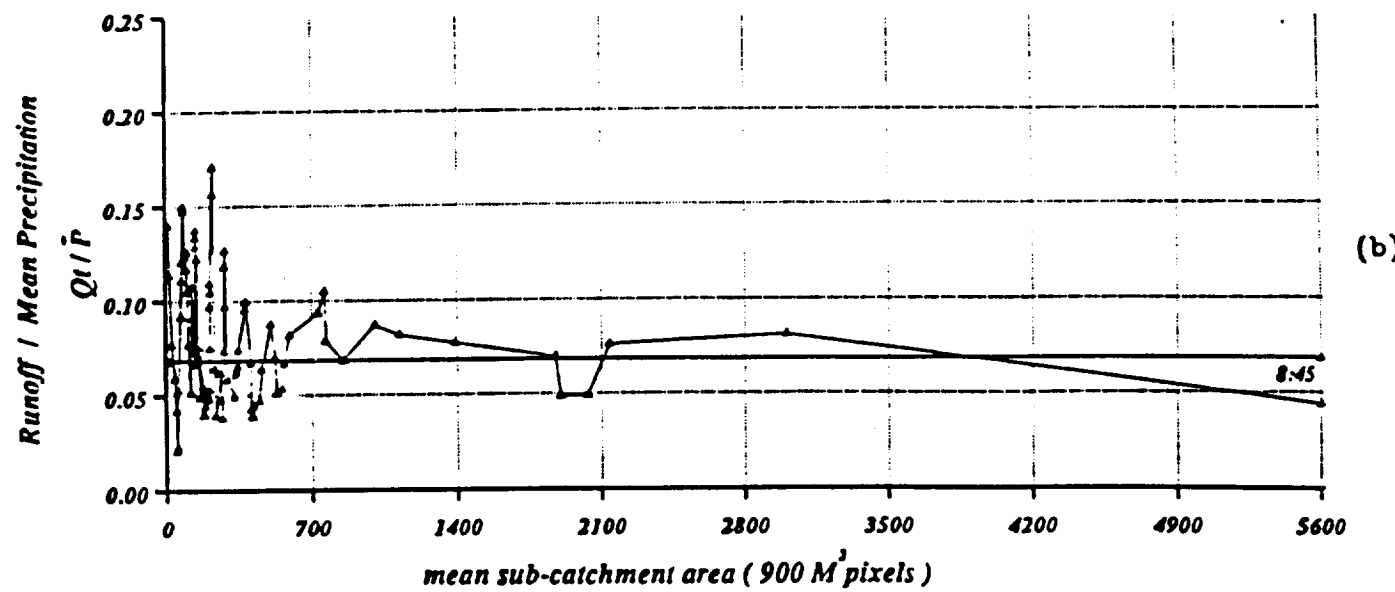
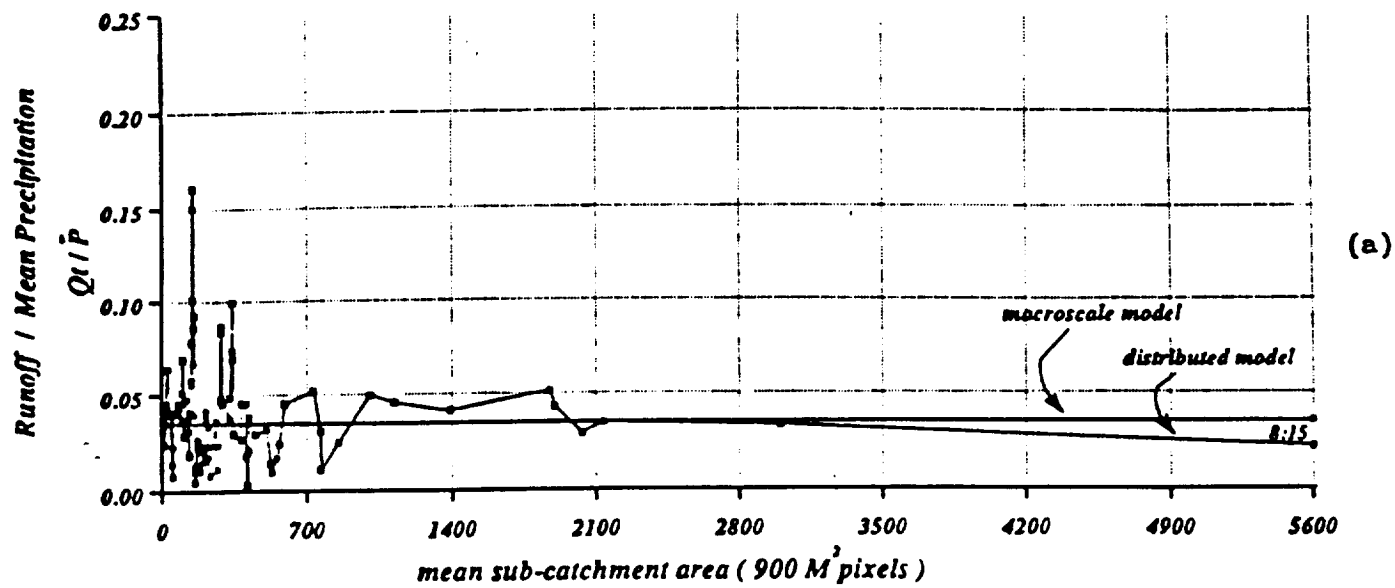


Figure 8: Comparison of storm runoff generated from the distributed model-a (see Appendix A) and from the macroscale water balance model (Equation A.6) for two time intervals on August 4, 1987: (a) 8:45 am, and (b) 9:30 am.

Modeled Interstorm Evaporation Following Rain Ending 01:30 July 18 1987

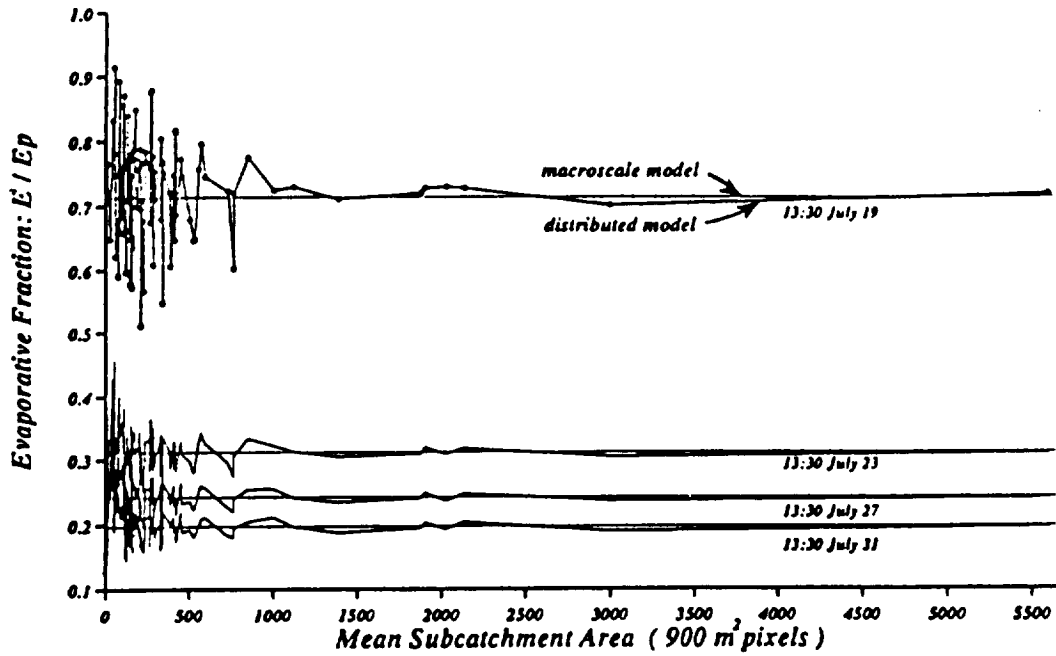


Figure 9: Comparison of interstorm evapotranspiration from the distributed model-a (see Appendix A) and from the macroscale water balance model (Equation A.7) for four times during the July 18 - 31, 1987 interstorm period.

RADAR IMAGE (July 10 45 hh l rad) / MAC-HYDRO Sub-Catchment area

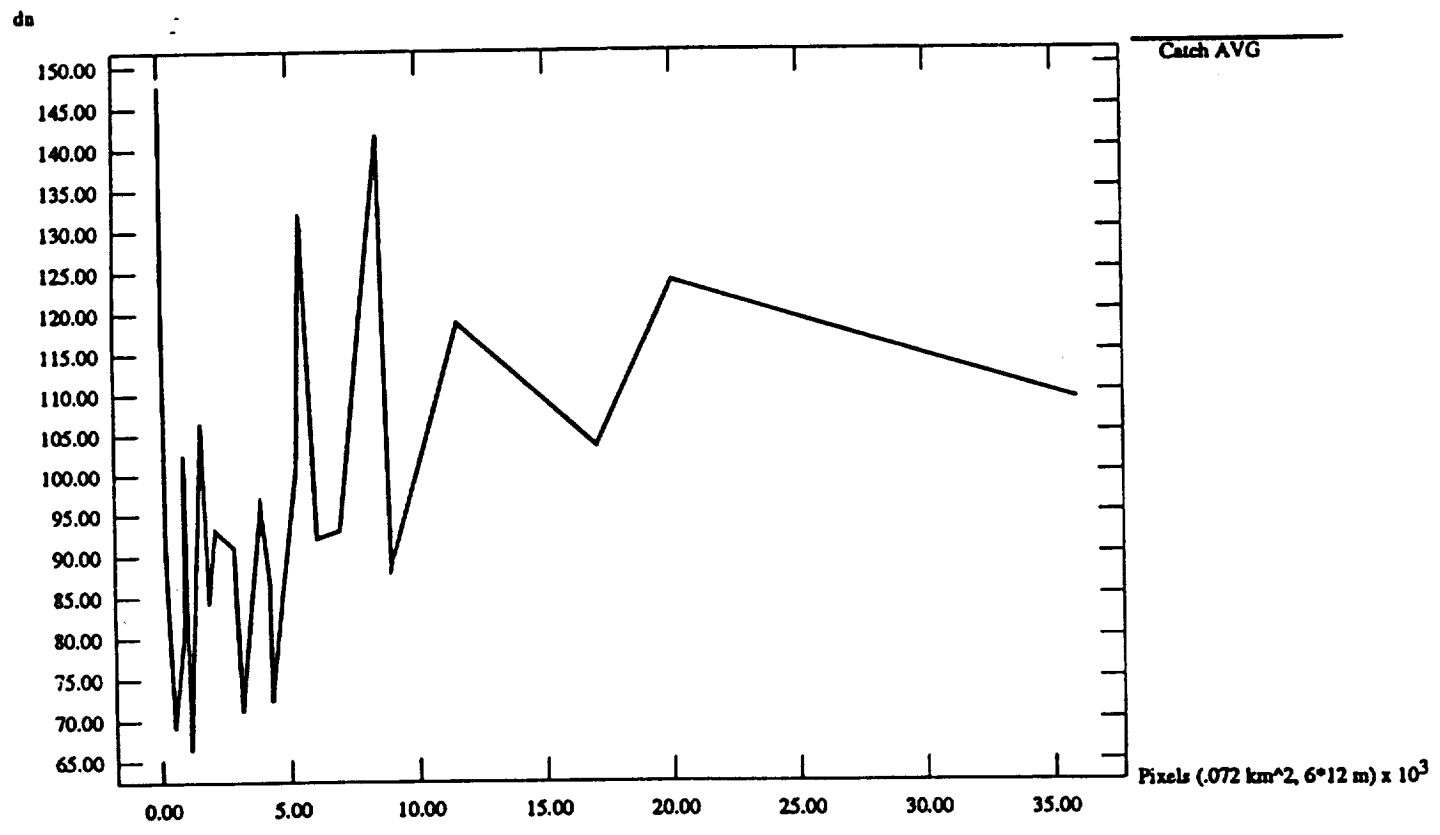


Figure 10: Comparisons of the average radar return (L-band, HH-polarization) in digital numbers for subcatchments within Mahantango Creek, PA. Data from the July 10, 1990 AIRSAR acquisition.

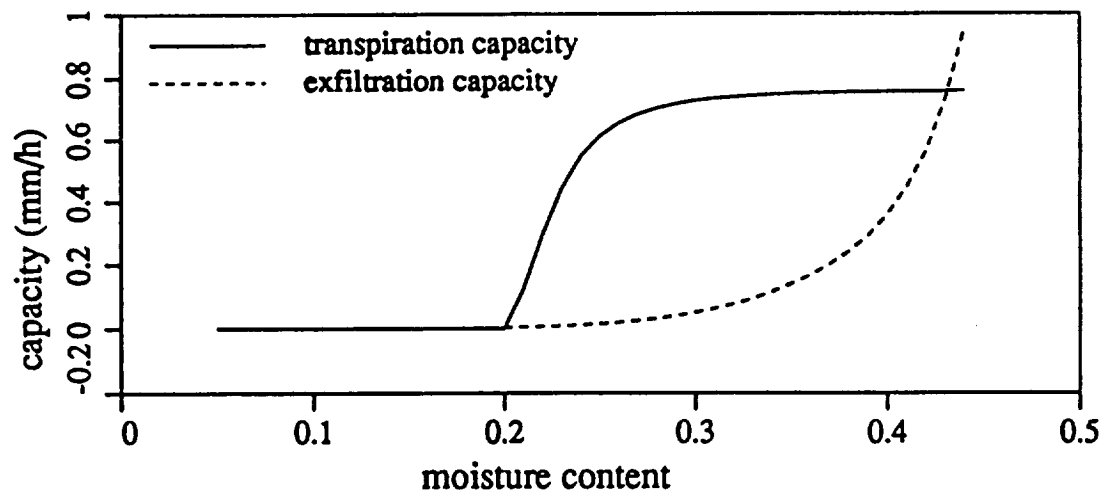


Figure 11: Transpiration and soil exfiltration capacities versus volumetric soil moisture content, after Famiglietti and Wood (1992a).

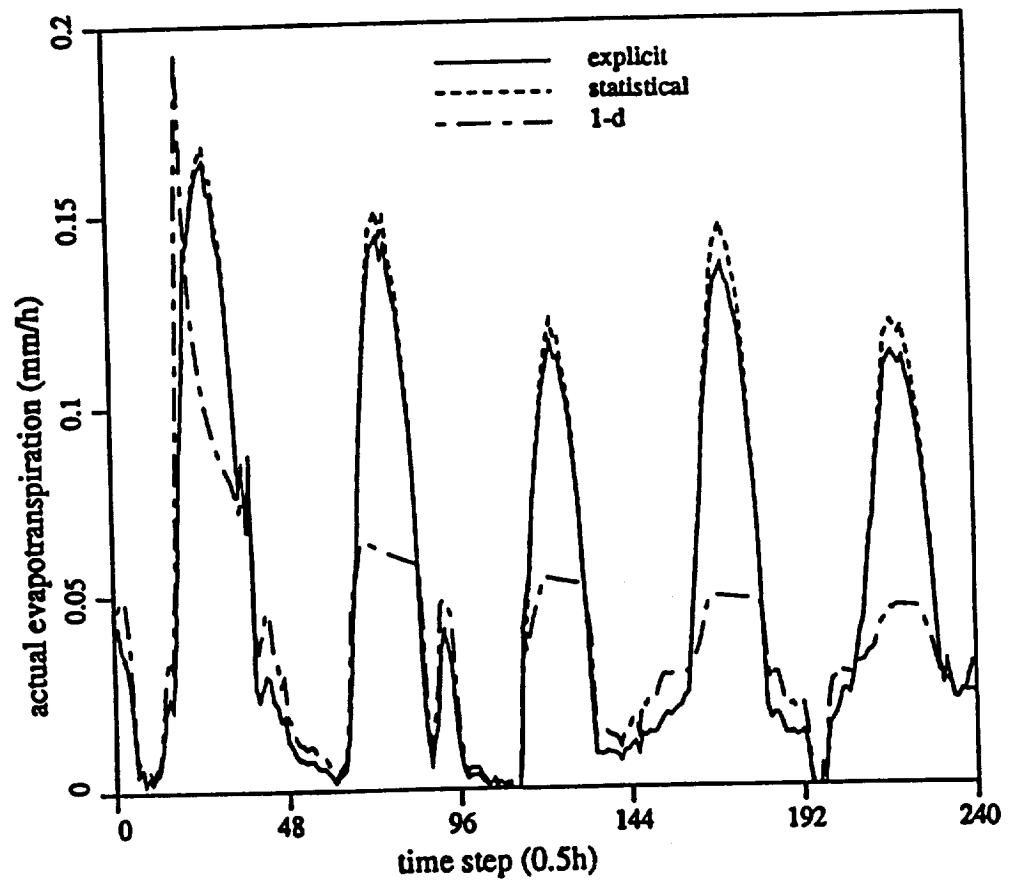
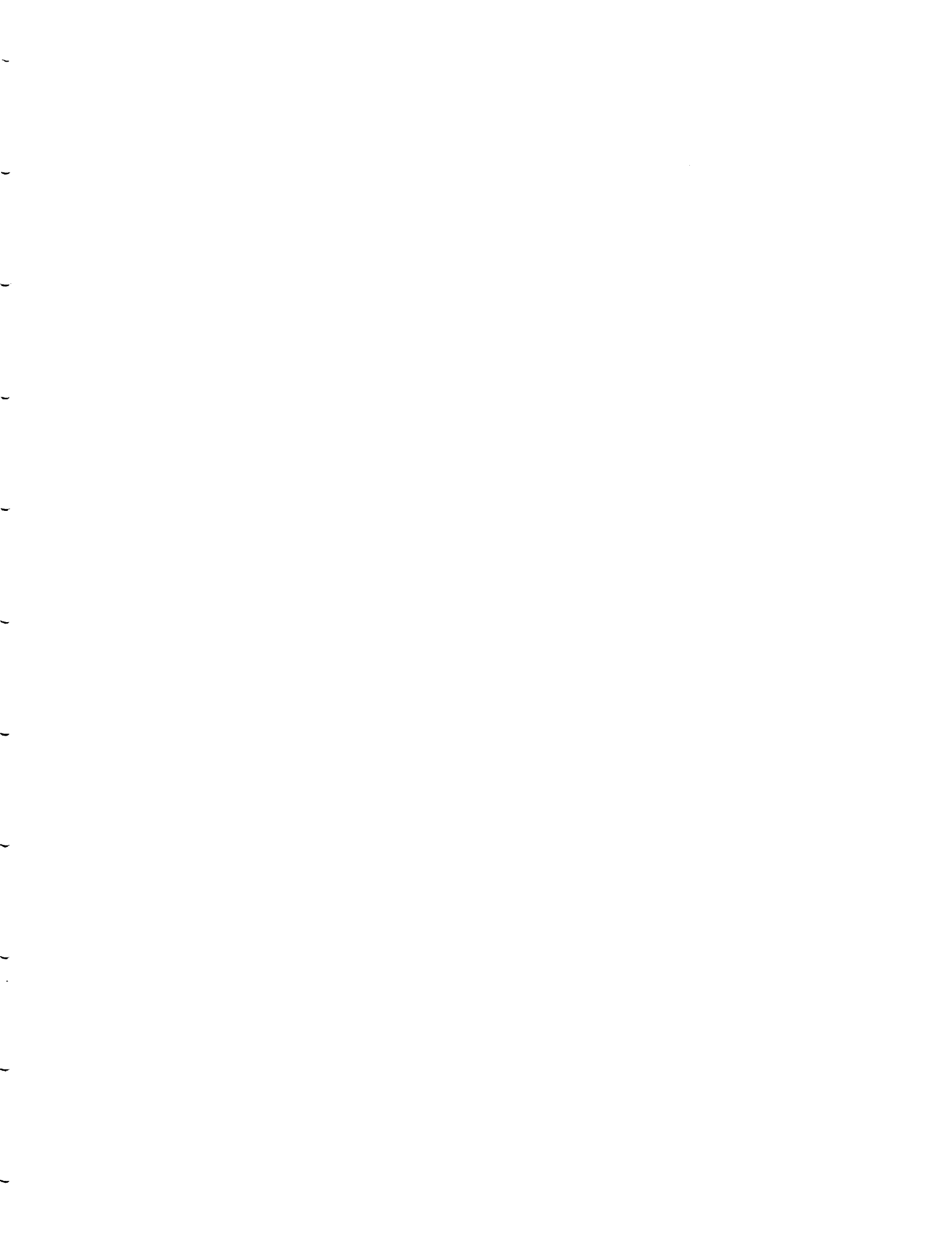


Figure 12: Computed catchment-average evapotranspiration from the distributed model-b (see Appendix A), the statistically aggregated macroscale model, and a lumped, one-dimensional model with spatially constant parameters. Results are for Kings Creek, KS for October 5-9, 1987.





Scaling Water and Energy Fluxes in Climate Systems: Three Land-Atmospheric Modeling Experiments

ERIC F. WOOD AND VENKATARAMAN LAKSHMI

Water Resources Program, Princeton University, Princeton, New Jersey

(Manuscript received on 25 October 1991, in final form 15 June 1992)

ABSTRACT

The effects of small-scale heterogeneity in land-surface characteristics on the large-scale fluxes of water and energy in the land-atmosphere system have become a central focus of many of the climatology research experiments. The acquisition of high-resolution land-surface data through remote sensing and intensive land-climatology field experiments (like HAPEX and FIFE) has provided data to investigate the interactions between microscale land-atmosphere interactions and macroscale models. One essential research question is how to account for the small-scale heterogeneities and whether "effective" parameters can be used in the macroscale models. To address this question of scaling, three modeling experiments were performed and are reviewed in the paper. The first is concerned with the land-surface hydrology during rain events and between rain events. The second experiment applies the Simple Biosphere Model (SiB) to a heterogeneous domain and the spatial and temporal latent heat flux is analyzed. The third experiment uses thematic mapper (TM) data to look at the scaling of the normalized vegetation index (NDVI), latent heat flux, and sensible heat flux through either scaling of the TM-derived fields using the TM data or the fields derived from aggregated TM data.

In all three experiments it was found that the surface fluxes and land characteristics can be scaled, and that macroscale models based on effective parameters are sufficient to account for the small-scale heterogeneities investigated. The paper also suggests that the scale at which a macroscale model becomes valid, the representative elementary scale (REA), is on the order 1.5–3 correlation lengths, which for land processes investigated appears to be about 1000–1500 m. At scales less than the REA scale, exact patterns of subgrid heterogeneities are needed for accurate small-scale modeling.

1. Introduction

The complex heterogeneity of the land surface through soils, vegetation, and topography, all of which have different length scales, and their interaction with meteorological inputs that vary with space and time result in fluxes of energy and water whose scaling properties are unknown. Research into land-atmospheric interactions suggests a strong coupling between land-surface hydrologic processes and climate (Charney et al. 1977; Walker and Rowntree 1977; Shukla and Mintz 1982; Rowntree and Bolton 1983; Shukla et al. 1990; Sud et al. 1990). The issue of "scale interaction" for land-surface-atmospheric processes has emerged as one of the critical unresolved problems for the parameterization of climate models.

Understanding the interaction between scales has increased in importance when the apparent effects of surface heterogeneities on the transfer and water and energy fluxes are observed through remote sensing and intensive field campaigns like HAPEX and FIFE (Sellers et al. 1988). The ability to parameterize macroscale models based on field experiments or remotely sensed

data has emerged as an important research question for programs such as the Global Energy and Water Experiment (GEWEX) or the Earth Observing System (EOS). It is also important for the parameterization of the macroscale land-surface hydrology necessary in climate models, and crucial to our understanding of how to represent subgrid variability in such macroscale models.

Current land-surface parameterization schemes can be put into three groups. The first is best represented by the bucket hydrology based on the work of Budyko (1956), which forms the basis for current long-term climate simulation. The second group would be the aggregated models with biospheric processes. This group of models is represented by the Biosphere Atmosphere Transfer Scheme (BATS) (Dickinson 1984) and the Simple Biosphere Model (SiB) (Sellers et al. 1986) in which the vertical structure of the canopy is well represented and the spatial characteristics are assumed constant. Wood (1991) has referred to these as "constant canopy" models. The final group incorporates subgrid heterogeneity at varying levels of detail, from fractional areas (Abramopolous et al. 1988) to statistical distribution for the subgrid processes (Entekhabi and Eagleson 1989; Famiglietti and Wood 1991a).

Corresponding author address: Eric F. Wood, Water Resources Program, Department of Civil Engineering and Operations Research, Princeton University, Princeton, NJ 08544.

Current research suggests two competing approaches for handling subgrid heterogeneity. (i) The first approach is based on the belief that subgrid processes have significant effect on processes at GCM scales and that the nonlinearity in subgrid-scale processes prevents simple scaling. This approach is supported by the observations of sea breezes arising from the significantly different characteristics between land and water. Avissar and Pielke (1989) also found that heterogeneity in land characteristics resulted in sea-breeze-like circulations and significant differences in surface temperatures and energy fluxes across the patches. It is important to note that in their hypothetical domain the patches are large with respect to the size of the domain. In natural domains the scale of such patches is often much smaller, which may lead to lower variability across the domain. (ii) The second approach is to ignore the variability in subgrid processes and to represent these processes at larger scales through models with effective parameters. Similarly, one may use aggregated inputs to drive these "macroscale" processes models at the large scale. This is essentially the approach of the constant-canopy biospheric models, where horizontal variability is ignored. It is also the approach of using small-scale micrometeorological field studies for calibration (Sellers and Dorman 1987; Sellers et al. 1989).

In this paper a series of numerical experiments are reported on that investigate the scaling of land-surface processes—either of the inputs or parameters—and compare the aggregated processes to the spatially variable case. Three experiments will be reported. These are as follows. The first is the aggregation of the hydrologic response in a catchment due to rainfall during a storm event and due to evaporative demands during interstorm periods. The second set of experiments is the spatial and temporal aggregation of latent heat fluxes, as calculated from SiB. The third set of experiments is the aggregation of remotely sensed land vegetation and latent and sensible heat fluxes using thematic mapper (TM) data from the FIFE experiment of 1987 in Kansas.

2. Aggregation of hydrologic responses

Runoff generation is now known to result from a complexity of mechanisms; during a particular storm different mechanisms may generate runoff from different parts of a catchment. As reviewed in Wood et al. (1990), these mechanisms include runoff due to rainfall on areas of low-permeability soils (referred to as the infiltration excess mechanism) and from rainfall on areas of soil saturated by a rising water table even in high-permeability soil (referred to as saturation excess runoff generation). These saturated contributing areas expand and contract during and between storm events.

As first shown by Beven and Kirkby (1979), variations in topography play a significant role in the spatial variation of soil moisture within a catchment, setting up spatially variable initial conditions for both runoff from rainstorms and evaporation during interstorm periods. Beven and Kirkby (1979) were the first to develop a saturated storm-response model (TOPMODEL). This model has been further expanded to include the above mechanisms (see Beven 1986a,b; Sivapalan et al. 1987). A complete description of the models, incorporating spatial variability in topography and soils, is provided in Wood et al. (1990) and will not be repeated here.

During interstorm periods, topography plays an important role in the downslope redistribution of soil moisture and, with soil properties, sets up the initial conditions for evaporation. The maximum evaporation rate is that rate demanded by atmospheric conditions, referred to as the potential rate, and this rate is met if the soil column can deliver the moisture to the surface. Rates lower than the potential rate will be at a "soil controlled" rate to be determined by soil properties and soil-moisture levels. The model with both storm and interstorm processes is fully described in Famiglietti et al. (1992).

The water-balance model described in Famiglietti et al. (1992) was applied to the Kings Creek catchment of the FIFE area in Kansas. Figure 1 shows the division of the 11.7 km² catchment into subcatchments—the number ranging from 5 to 66 depending on the scale. All subcatchments represent hydrologically consistent units, in that runoff flows out of the subcatchment through one flow point and that the surface-runoff flux across the other boundaries is zero.

For a rainfall storm on 4 August 1987, the average runoff for the subcatchments was calculated for two times and plotted in Fig. 2 against a subcatchment area measured in pixels. Each pixel is 900 m². Notice that the runoff Q_i is normalized by the average precipitation, \bar{P} . The same type of plot was done for selected times during an interstorm period that extended from 18 July through 31 July 1987 and is presented as Fig. 3. The behavior of the catchment shows that at small scales there is extensive variability in both storm response and evaporation. This variability appears to be controlled by variability in soils and topography whose length scales are on the order of 10²–10³ m—the typical scale of a hill slope. With increased scale, the increased sampling of hill slopes leads to a decrease in the difference between subcatchment responses. At some scale, the variance between hydrologic responses for catchments of the same scale should reach a minimum (Wood et al. 1990). Wood et al. (1988) suggest that this threshold scale represents a representative elementary area (REA), which is proposed to be the fundamental building block for hydrologic modeling, as defined in Wood et al. (1988) and Wood et al. (1990).



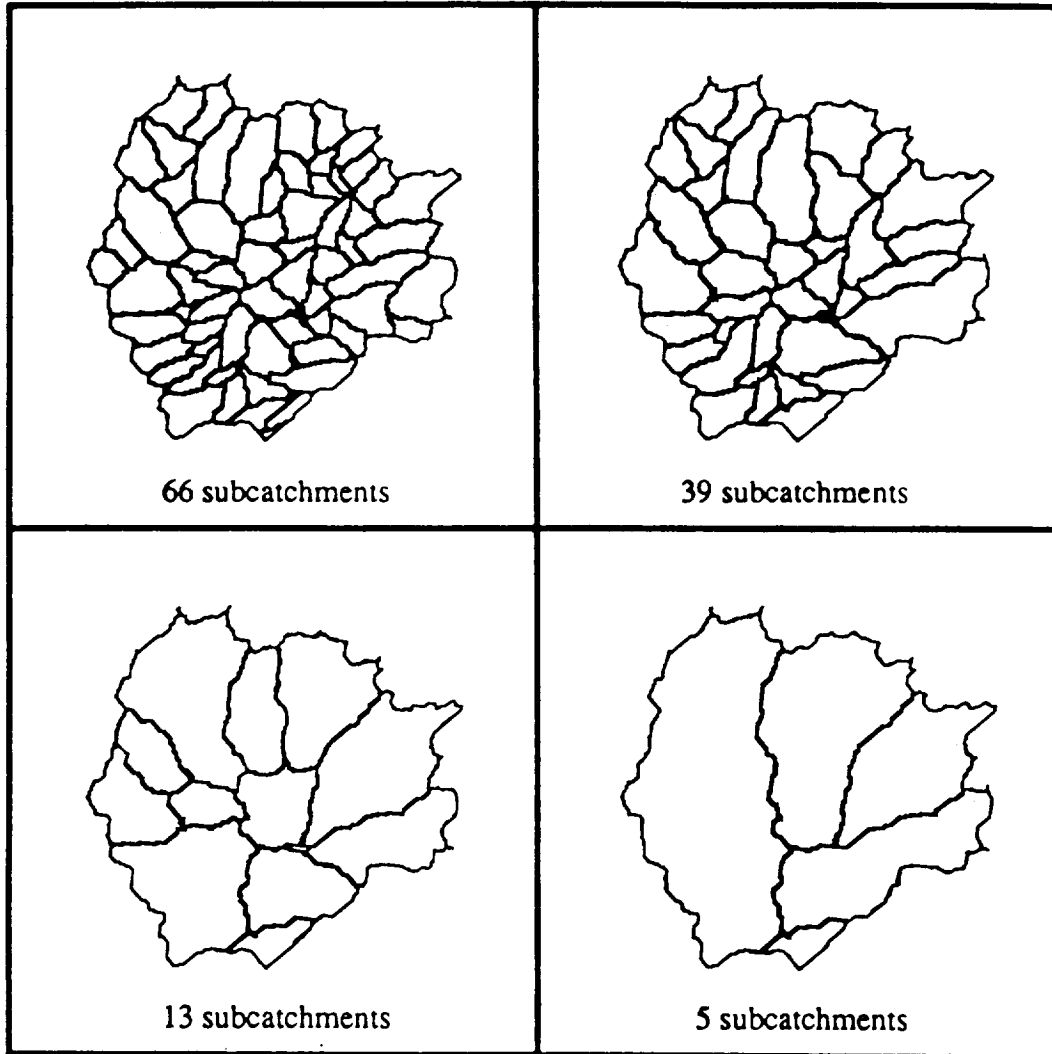


FIG. 1. Natural subcatchment divisions for Kings Creek, Kansas.

The REA is the critical scale at which implicit continuum assumptions can be used without explicit knowledge of the actual patterns of topographic, soil, or rainfall fields. It is sufficient to represent these fields by their statistical characterization.

By inspecting Figs. 2 and 3, it appears that the size of the REA is on the order of 1 km^2 (about 1000–1200 pixels, each of which are 900 m^2). The results also suggest that at larger scales it would be possible to model the responses using a simplified macroscale model based on the statistical representation of the heterogeneities in topography, soils, and hydrologic forcings (rainfall and potential evaporation). To date, only a limited range of catchments has been analyzed, all having moderate topography and located in regions with humid climates. The REA scale appears to be quite consistent at about $1\text{--}2 \text{ km}^2$ and to be the same

scale for both runoff and evaporation processes. Clearly, additional catchments representing a broader range of climates and catchment sizes need to be analyzed before definitive statements concerning the REA scale can be made.

Using the statistical distribution of the topographic-soil index, one can determine the fraction of the catchment that will be saturated due to the local soil storage being full. These areas will generate saturation excess runoff at the rate \bar{p} , the mean rainfall rate. For that portion of the catchment where infiltration occurs, the local expected runoff rate at time t , m_q , can be calculated as the difference between the mean rainfall rate, \bar{p} , and the local expected infiltration rate, m_g . This implies that m_q and m_g are *conditioned* upon a topographic-soil index whose statistical distribution is central to the REA macroscale model. The difference be-

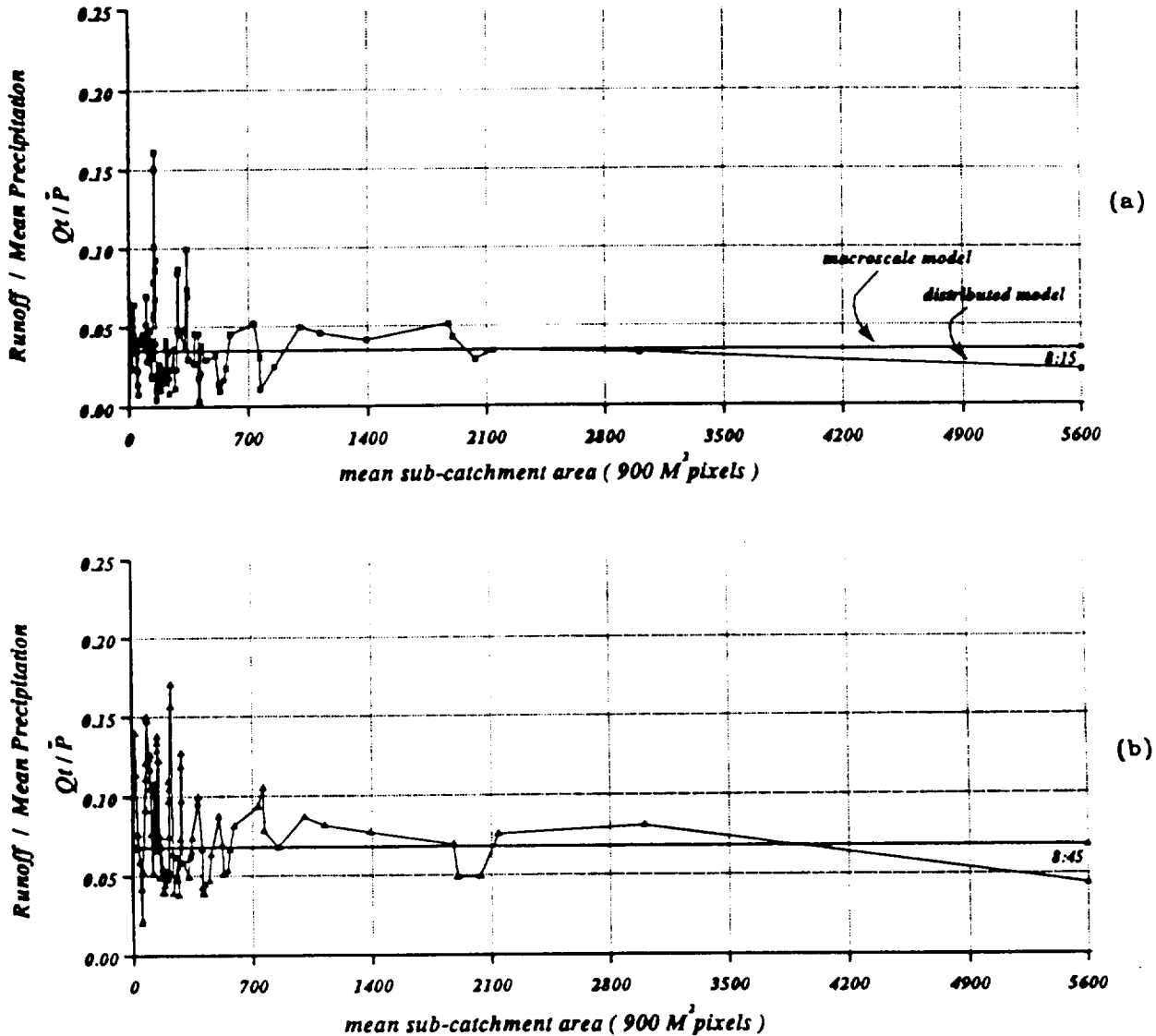


FIG. 2. Comparison of storm runoff generated from the distributed model and from the macroscale water-balance model for two time intervals on 4 August 1987: (a) 0845 LDT and (b) 0930 LDT.

tween averaged rainfall and infiltration can be expressed as

$$m_q[t|\ln(aT_e/T_i \tan\beta)] = \bar{p} - m_g[t|\ln(aT_e/T_i \tan\beta)], \quad (1)$$

where $\ln(aT_e/T_i \tan\beta)$ is the topographic-soil index for a location i in the catchment and is a function of α , the contributing area upslope to i ; $\tan\beta$, the local slope angle; T_i , the soil transmissivity at i ; and T_e , the catchment average of T_i . As discussed above, m_q and m_g are time-varying functions whose values at any particular time are equal for points within the catchment

having the same topographic-soil index; this dependence is indicated in Eq. (1) by the $|\cdot$. The full development of the topographic-soil index is provided in Beven and Kirkby (1979), Beven (1986a,b), Sivapalan et al. (1987), and Wood et al. (1990). Both the local expected runoff rate and the local expected infiltration rate are (probabilistically) conditioned on the topographic-soil index, $\ln(aT_e/T_i \tan\beta)$. The runoff production from the catchment is found by integrating, usually numerically, the conditional rate over the statistical distribution of topographic-soil index. Figure 2 also gives results for the macroscale model along with the distributed model. Since the macroscale model is scale invariant, it appears as a straight line in Fig. 2.

Modeled Interstorm Evaporation Following Rain Ending 01:30 July 18 1987

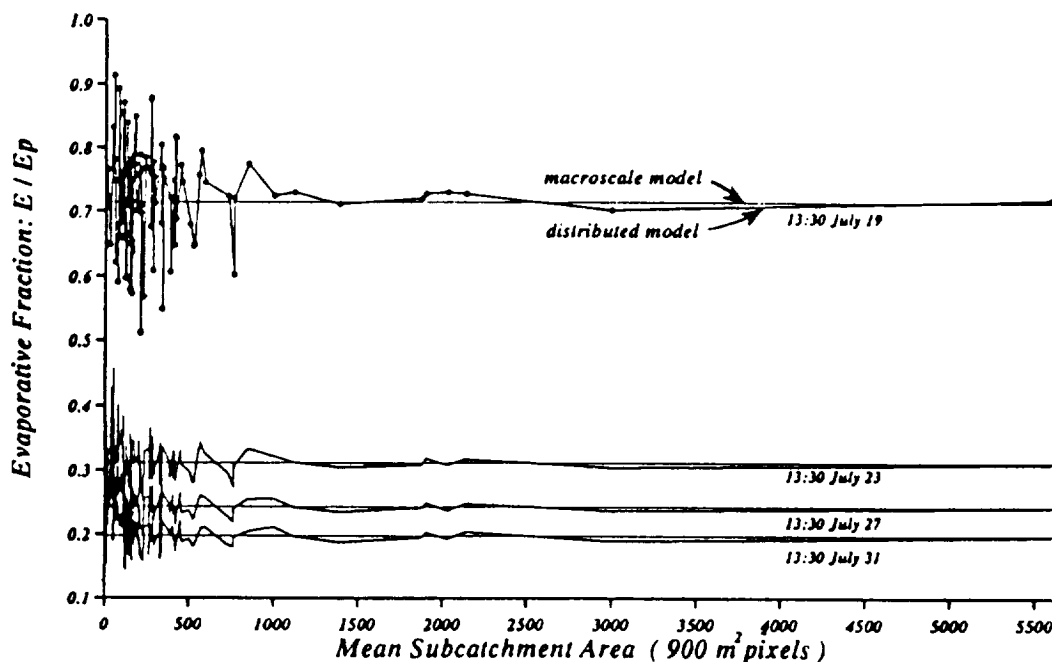


FIG. 3. Comparison of interstorm evapotranspiration from the distributed model and from the macroscale water-balance model for four times during the 18–31 July 1987 interstorm period.

In a similar way, a macroscale evaporation model is developed for interstorm periods. As stated earlier, topography plays an important role in the interstorm redistribution of soil moisture. Variations in soil properties and topography lead to variations in soil moisture and the initial conditions for the evaporation calculations. For those portions of the catchment for which the soil column can deliver water at a rate sufficient to meet the potential evapotranspiration or atmospheric demand rate E_p , the actual rate E equals E_p ; otherwise, the rate will be at a lower soil-controlled rate E_s . Within the TOPMODEL framework, locations with the same value of the topographic-soil index will respond similarly, implying a macroscale model conditioned on that index. The macroscale model can be written as:

$$m_E [t | \ln(aT_e/T_i \tan\beta)] = \min\{m_{E_s}, [t | \ln(aT_e/T_i \tan\beta)], \bar{E}_p(t)\}, \quad (2)$$

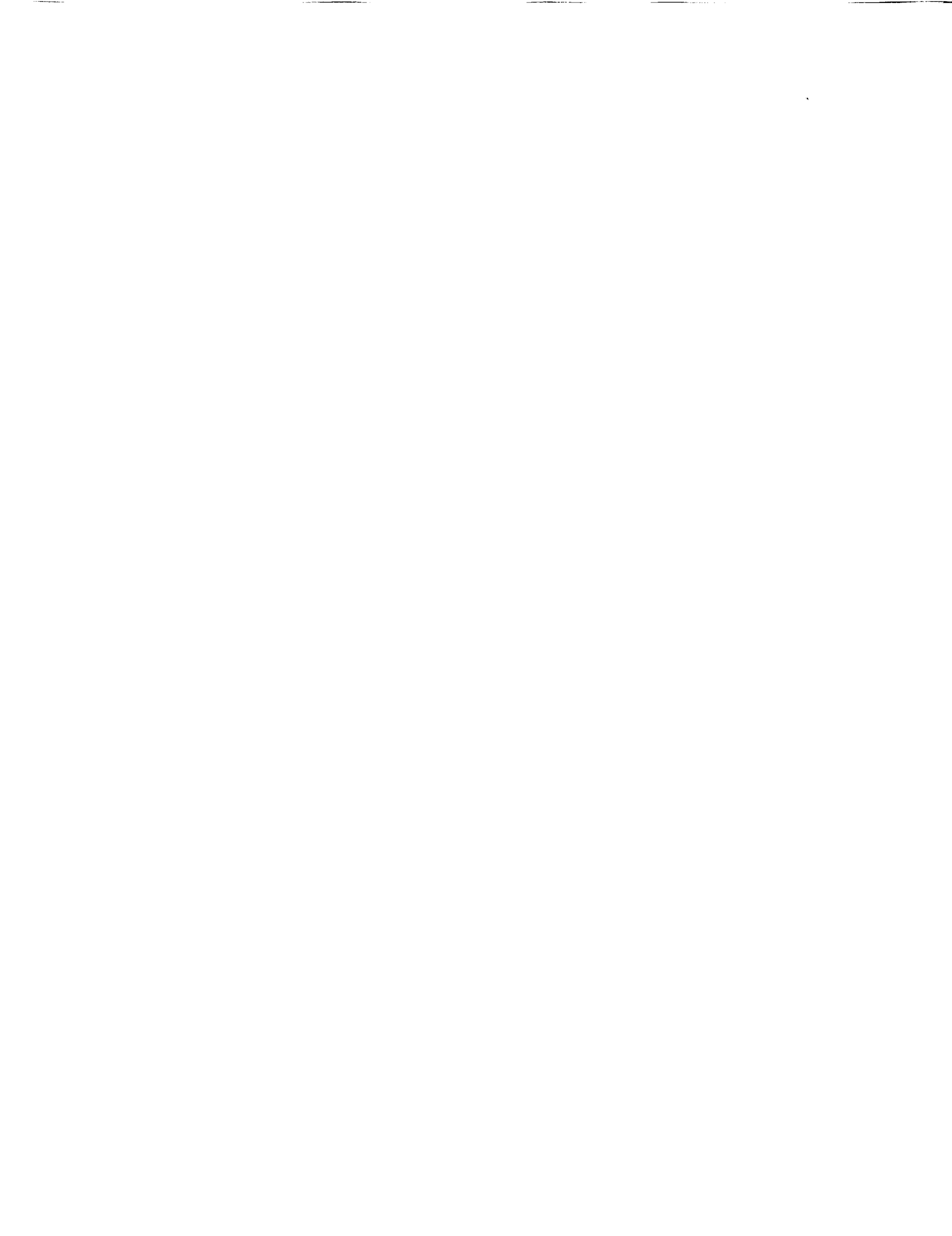
where m_E refers to the mean evaporation rate at locations in the catchment with the same index, m_{E_s} refers to the mean soil-controlled rate, and \bar{E}_p to the spatially average potential or atmospheric demand rate. Figure 3, which compares the evaporation rates from the distributed model across the range of scales for Kings Creek, also includes the derived rates from the macroscale evaporation model. As in Figure 2, the macroscale model is scale invariant and appears as a straight line.

a. Summary on hydrological scaling

The results from the REA analysis suggest that progress has been made in understanding the transition in hydrologic responses during storm and interstorm periods as scale is increased in the presence of spatial variability. In particular, the results indicate that the macroscale models that preserve the statistical characterization of the small-scale variability in the hydrologic controls (topography and soils) can accurately represent both storm and interstorm water fluxes. The results presented here are based on a specific model applied to the FIFE study site. Good agreement between model predictions and observations have been obtained (see Famiglietti and Wood 1991b; Famiglietti et al. 1992). The model representation of soil water movement (infiltration and evapotranspiration) is highly nonlinear, so we are confident that the scaling of these processes across a range of heterogeneous hill slopes and soils, which leads to the macroscale model, is reasonable. Nonetheless, the results presented here need to be expanded over a wider range of catchment and climatic scales to further verify the concepts of the representative elementary area.

3. Spatial and temporal scaling using a biospheric transfer model

The development of models that have biospheric-atmospheric interactions is motivated by recent ad-



ATMOSPHERIC BOUNDARY LAYER

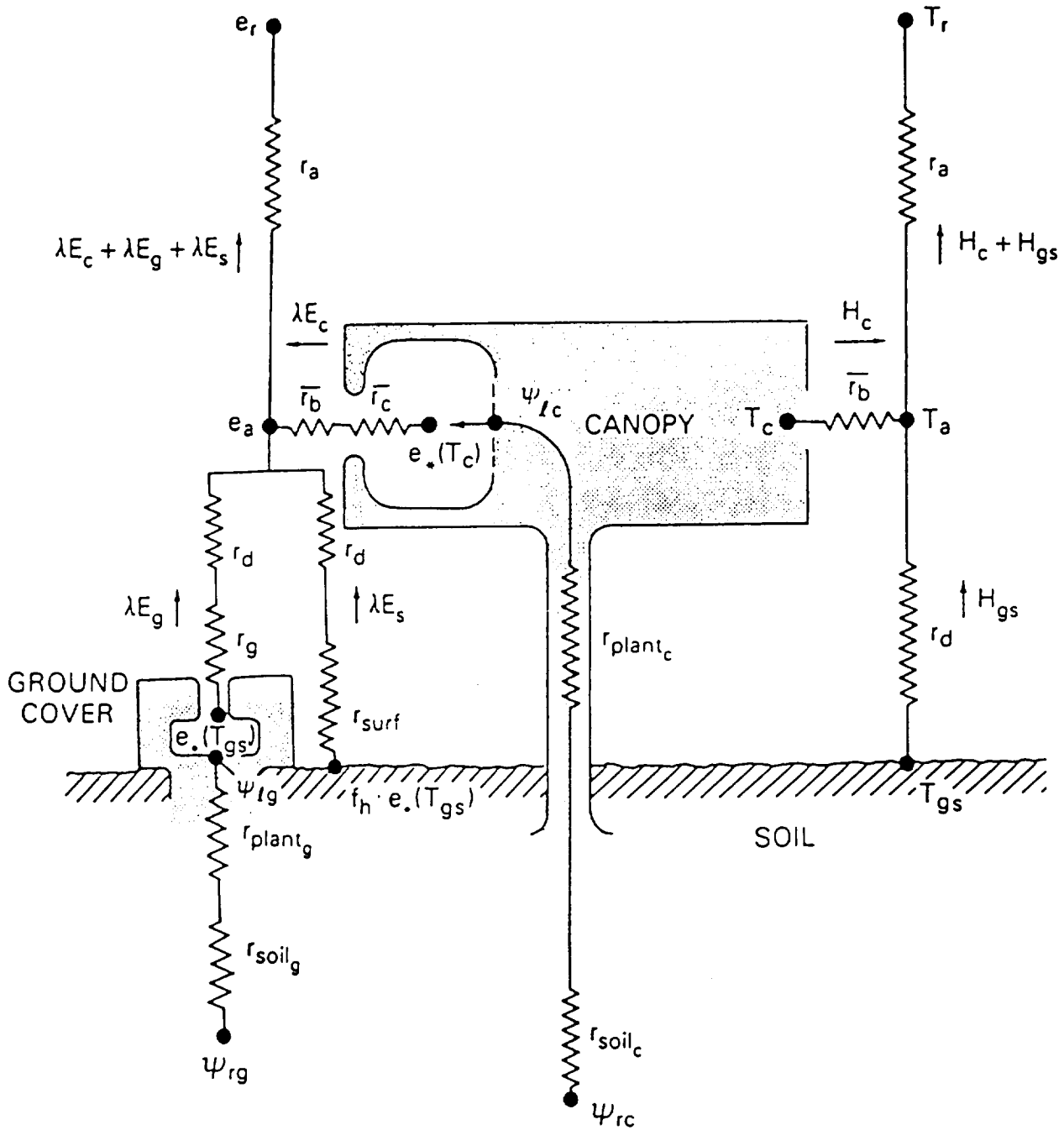


FIG. 4. Framework of the Simple Biosphere Model (SiB). The transfer pathways for the latent and sensible heat fluxes are shown on the left- and right-hand sides of the diagram, respectively. The treatment of radiation and intercepted water has been omitted for clarity. Symbols are as defined in Sellers et al. (1986) [from Sellers et al. (1986)].

vances in plant physiology, micrometeorology, and hydrology and our ability to integrate all of these small-scale physical processes that control biosphere-atmo-

sphere interactions. Two of the most widely used models are the Simple Biosphere Model (SiB) (Sellers et al. 1986) and the Biosphere-Atmosphere Transfer



Scheme (BATS) Model (Dickinson et al. 1986). The models attempt to separate the vegetation canopy from the soil surface and to represent the energy and water fluxes from the canopy in detail. Thus, the resulting models have a complex representation of the soil-vegetation-atmosphere system, which gives them the appearance of having tremendous vertical resolution and structure. On the horizontal scale, these models usually assume homogeneous conditions; that is, the parameters for the soil and vegetation properties are assumed constant within a GCM grid, thus ignoring spatial heterogeneity. This has led to describing these models as "big-leaf" or "constant-canopy" models.

Figure 4 gives a schematic for the parameterization of SiB. As described by Sellers et al. (1986), the parameterization consists of a two-layer vegetation canopy whose elements and roots are assumed to extend

uniformly throughout the GCM grid. From the prescribed physical and physiological properties of the vegetation and soil, the model calculates (i) the reflection, transmission, absorption, and emission of direct and diffuse radiation in the visible, near-infrared, and thermal wavelength intervals; (ii) the interception of rainfall and its evaporation from leaf surfaces; (iii) the infiltration, drainage, and storage of residual rainfall in the soil; (iv) the control of photosynthetically active radiation and the soil-moisture potential, inter alia, over the stomatal functioning and, thereby, over the return transfer of the soil moisture to the atmosphere through the root-stem-leaf system of the vegetation; and (v) the aerodynamic transfer of water vapor, sensible heat, and momentum from the vegetation and the soil to a reference level within the atmospheric boundary layer. The model originally had seven prog-

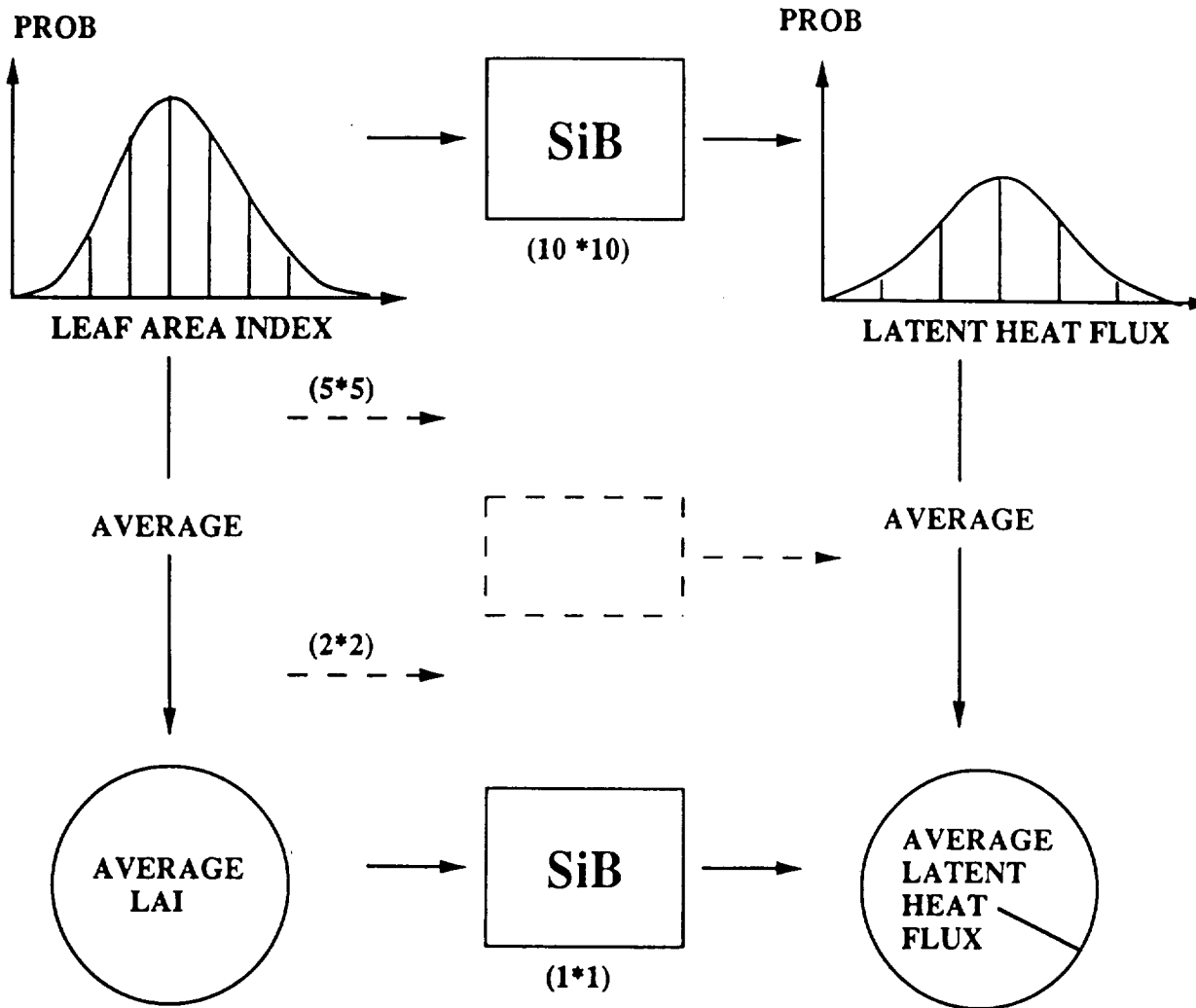


FIG. 5. Schematic diagram for the biosphere-atmosphere scaling experiment. The spatially variable inputs and derived outputs are shown on the left- and right-hand sides of the diagram, respectively. Low aggregation to high aggregation of inputs are shown from top to bottom, respectively.



nostic physical-state variables: two temperatures (a canopy temperature and ground temperature), two interception water storages (one for the canopy and one for the ground cover), and three soil-moisture storages of which two are for the two classes of vegetation and one for the soil recharge layer (Sellers et al. 1986). Recently an eighth prognostic variable was added for following the deep-soil temperature. SiB has been tested in a climate model by Sato et al. (1989) in which SiB is compared to the bucket model land-surface parameterization.

To investigate the effect of subgrid variability on the scaling of latent heat fluxes as derived from SiB, the following numerical experiment was carried out. A gridded domain was defined in which the vegetation density (as described by its leaf-area index), precipitation, and initial soil wetness were allowed to be spatially variable. At the finest scale, a 10×10 grid, the scale of the grid (L_G) divided by the scale of the domain (L_D) is 0.1. The average parameters for the domain were based on a calibration of SiB for data collected in Amazonia and reported in Sellers et al. (1989). The data consisted of 43 days of meteorological observations at a 1-h time interval.

The scaling analysis is presented schematically in Fig. 5. While all three variables were allowed to vary, Fig. 5 is simplified to show only the leaf-area index. Within the 10×10 domain, the random field for the spatially variable parameter is generated from a normal distribution with coefficient of variation of 0.25. For the results presented here, spatial correlation was not included. SiB can then be run for each grid. This structure ignores any horizontal interaction among grids. From the 10×10 SiB runs, the probability distribution for the latent heat flux can be constructed.

Spatial scaling is investigated by averaging the inputs (leaf-area index, initial soil wetness, and rainfall) from adjacent grids. The levels considered were aggregated domains having L_G/L_D ratios of 0.2 (a 5×5 gridded domain), $L_G/L_D = 0.5$, and $L_G/L_D = 1.0$; the latter case being the spatially average, homogeneous case. Comparisons can be made between the derived latent heat fluxes from the aggregated inputs (the left-hand side of Fig. 5) and the averaging of the 10×10 (detailed) domain. If the inputs operate within SiB in a highly nonlinear manner, then the two averaging schemes would lead to a significant difference. The spatially averaged inputs would be biased compared to the spatially distributed parameter case.

Figure 6 shows the 43-day mean latent heat flux across the range of aggregations. In Fig. 6a, only the leaf-area index is varied, while all three inputs are varied in 6b. Figure 7 presents a scatterplot comparison between the hourly latent heat fluxes averaged over the 10×10 grid domain and the fluxes derived from the averaged inputs.

Three observations are in order. At the finest scale,

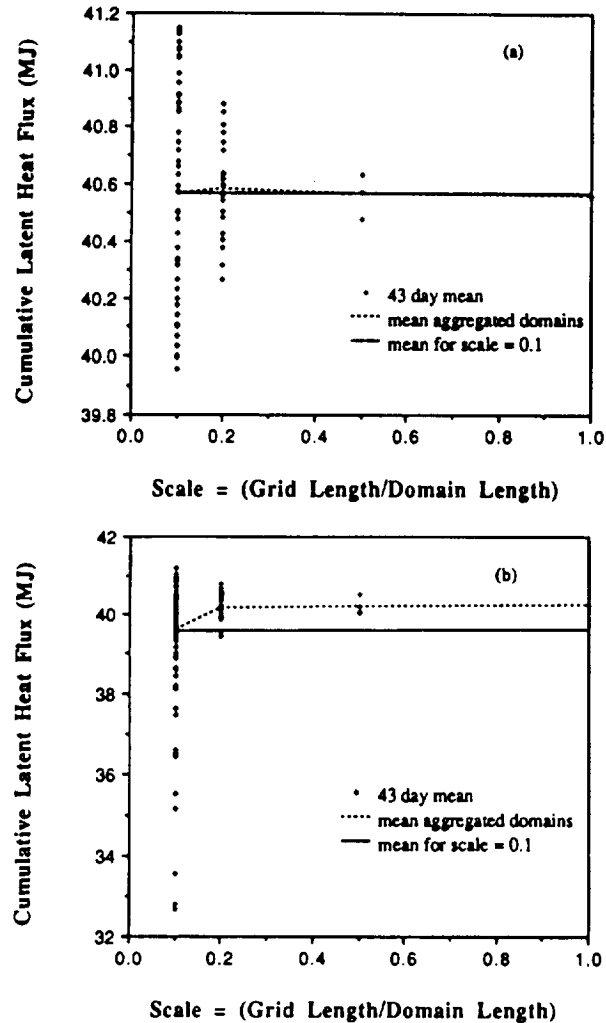


FIG. 6. Comparisons of latent heat fluxes, derived using SiB, over a range of domain scales: (a) leaf-area index (LAI) spatially variable and (b) LAI, rainfall, and initial soil moisture variable. The fluxes were modeled using data from Sellers et al. (1989) and are shown as cumulative fluxes over 43 days.

$L_G/L_D = 0.1$, there is substantial variability across the grids compared to the higher levels of aggregation. Nonetheless, the absolute range of variability is very small, given what we feel is a realistic range for the input variability. For the hourly data presented in Fig. 7, the range of variability due to lumping is extremely small when compared to the range of calculated latent heat fluxes over the observation period. Second, a small bias is observed for the case where all three parameters are varying. This bias is due to the variability in initial soil wetness, the input parameter that appears to have the greatest influence on the average latent heat flux. Finally, we believe that the REA concept appears to hold for these experiments and is about $L_G/L_D = 0.2$. In fact, subsequent analysis shows that the REA is re-



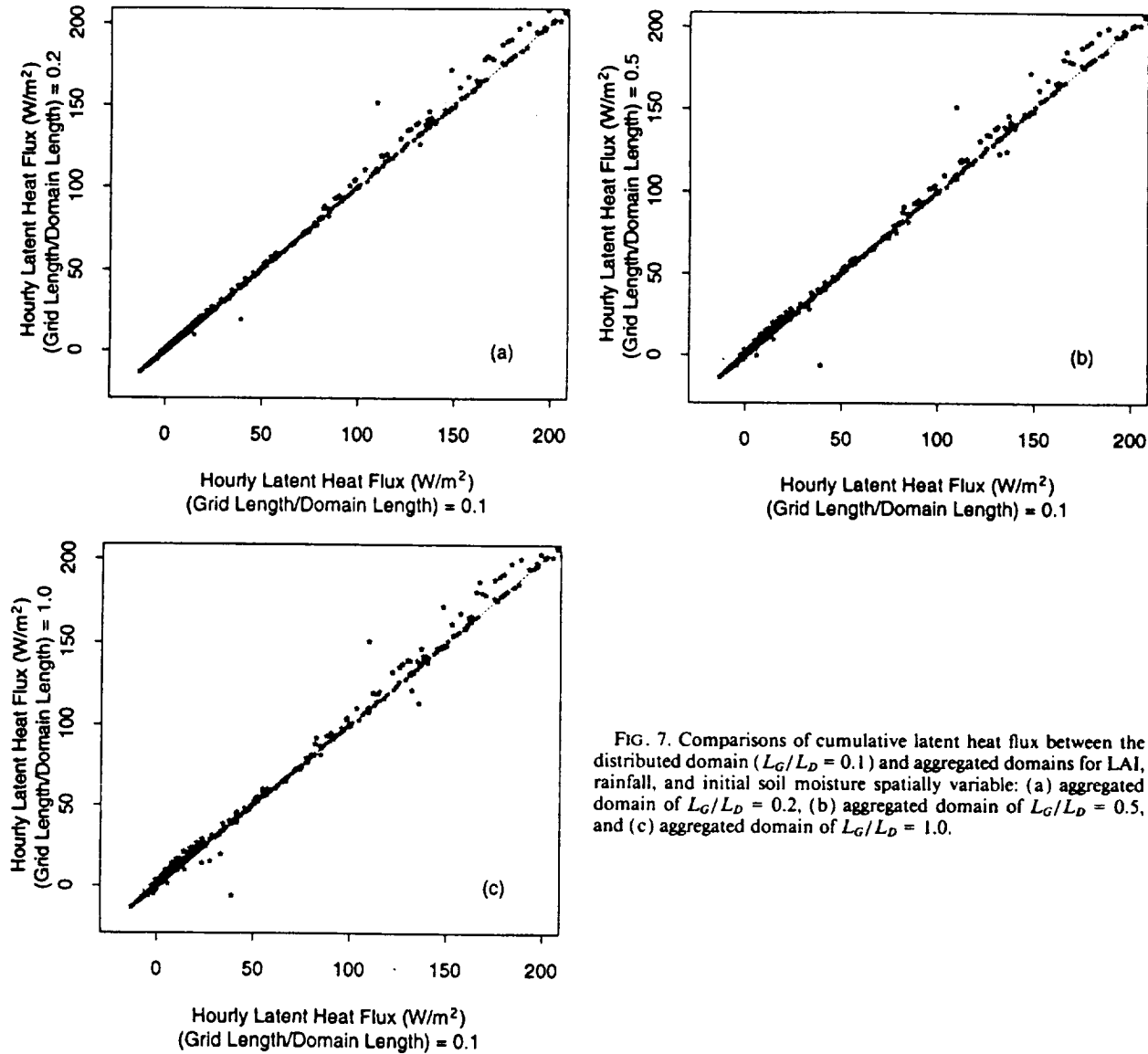


FIG. 7. Comparisons of cumulative latent heat flux between the distributed domain ($L_G/L_D = 0.1$) and aggregated domains for LAI, rainfall, and initial soil moisture spatially variable: (a) aggregated domain of $L_G/L_D = 0.2$, (b) aggregated domain of $L_G/L_D = 0.5$, and (c) aggregated domain of $L_G/L_D = 1.0$.

lated to the correlation length of the subgrid heterogeneities. Increased spatial correlation in the parameters leads to larger REAs. Further field studies are needed to establish realistic correlation lengths for these parameters.

The results presented in Figs. 6 and 7 used rainfall data at a temporal resolution of 1 h. The effect of temporal averaging is shown in Fig. 8 with a scatterplot of the latent heat fluxes, as computed using hourly rainfall, and temporally averaged at either 2 h or 24 h. The effect is a strong bias and variability between the two aggregation schemes. This demonstrates that temporal averaging of the rainfall input (which results in a reduction of rainfall intensity) has a significant impact on the surface water balance (runoff, soil moisture) and subsequent latent heat fluxes.

4. Scaling TM-derived surface variables

The earlier two numerical experiments were concerned with scaling hydrologic and energy fluxes using a water-balance and land-surface biospheric model. In this third experiment, high-resolution thematic mapper (TM) satellite data were used to derive the normalized difference vegetation index (NDVI), latent heat, and sensible heat fluxes for the 15 August 1987 overpass. The resolution of TM is 30 m for bands 1 through 5, and 120 m for the thermal band that was used for the sensible and latent heat flux calculations.

The scaling question investigated here is whether averaging the TM bands prior to calculating NDVI or the fluxes provides the same derived quantities as would be found by calculating the quantities at the TM res-

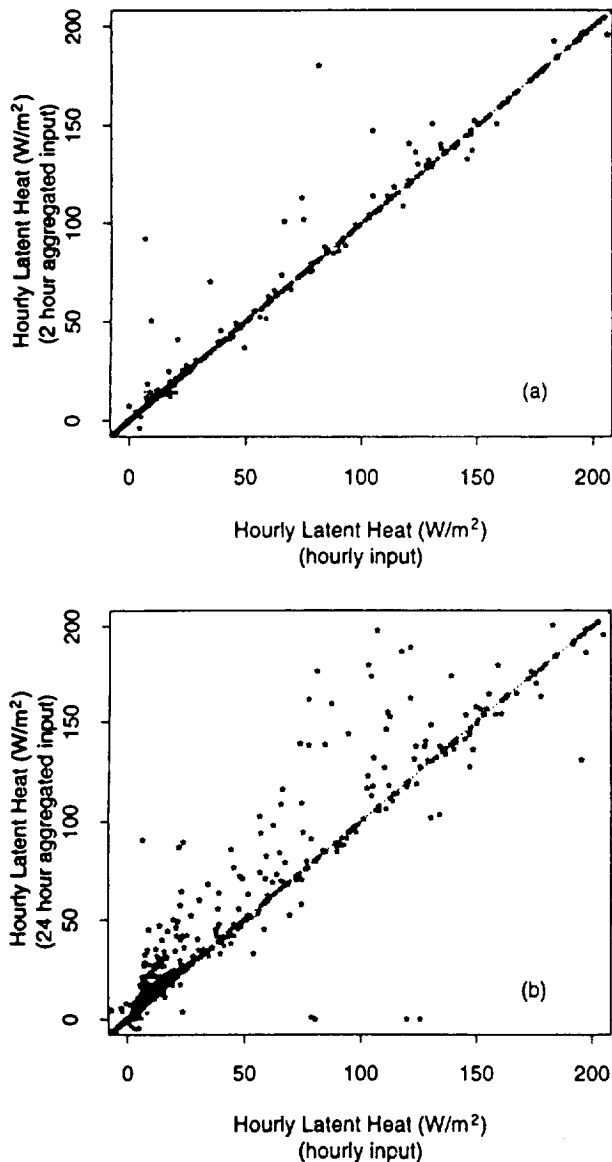


FIG. 8. Comparisons of cumulative latent heat flux between hourly rainfall and temporally averaged rainfall: (a) rainfall aggregated over 2 h, (b) rainfall aggregated over 24 h. The variables: LAI, rainfall, and initial soil moisture are spatially constant.

olution and averaging. The equivalence of the two approaches depends on the degree of nonlinearity represented by functions that relate NDVI and fluxes to TM data.

a. Scaling NDVI

The following procedure was followed: the normalized difference vegetation index (NDVI) was calculated at the 30-m TM resolution using

$$\text{NDVI} = \frac{(B_4 - B_3)}{(B_4 + B_3)}, \quad (3)$$

where B_3 represents band 3 (0.63–0.69 μm), and B_4 represents band 4 (0.76–0.90 μm). The first is often referred to as the red and the latter the near-infrared band. The NDVI image corresponding to a TM scene acquired over the FIFE area for 15 August 1987 is given in Fig. 9. The TM scene was fully calibrated before the calculations were carried out.

At aggregated scales, two procedures were followed. One was to spatially aggregate the TM bands and then use Eq. (3), while the second procedure is to spatially aggregate the NDVI based on the 30-m TM data. Figure 10 shows the aggregated NDVI, using the second procedure, for aggregation levels of 300×300 m, 750×750 m, and 1500×1500 m. A resolution equivalent to AVHRR would lie between the last two cases. Comparisons between the two aggregation procedures can best be shown by a scatterplot between the aggregated 30-m-based NDVI and the NDVI derived using aggregated TM bands; these comparisons are presented in Fig. 11.

One striking observation arises from comparing Figs. 9 through 11. Notice that the detailed structure observable in Fig. 9 is lost in Fig. 10, and yet the averaged NDVI from the two aggregation schemes are essentially the same as can be seen in scatterplot of Fig. 11. Figure 11 does show that a small bias exists between the two aggregation procedures but its magnitude is rather insignificant. These results indicate that NDVI calculated from spatially averaged TM (or lower-resolution AVHRR data) will be equivalent to the NDVI scaled up from the full-resolution image.

b. Scaling up TM-derived latent and sensible heat fluxes

Latent and sensible heat fluxes over the FIFE area during 15 August 1987 were estimated using the thematic mapper (TM) thermal band (10.45–12.5 μm , with a resolution of 120 m) aboard Landsat 5 and a procedure presented by Holwill and Stewart (1992). The Landsat overflight was at 1632:50 UTC and the fluxes estimated for 1600–1700 UTC. The relationship between surface radiometric temperature and emittance is given for the Landsat thermal channel by Markham and Barker (1986) as

$$T_s = K_2 / \ln(K_1 / R_s + 1), \quad (4)$$

where R_s is surface emittance in ($\text{W m}^{-2} \text{Sr}^{-1} \mu\text{m}^{-1}$), K_1 and K_2 are coefficients that, after atmospheric calibration for 15 August 1987, have values of $K_1 = 607.76 \text{ W m}^{-2} \text{Sr}^{-1} \mu\text{m}^{-1}$ and $K_2 = 1260.56 \text{ K}$ (Goetz 1991, personal communication).

The procedure developed by Stewart and Holwill (1992) combines the spatial TM thermal data with data

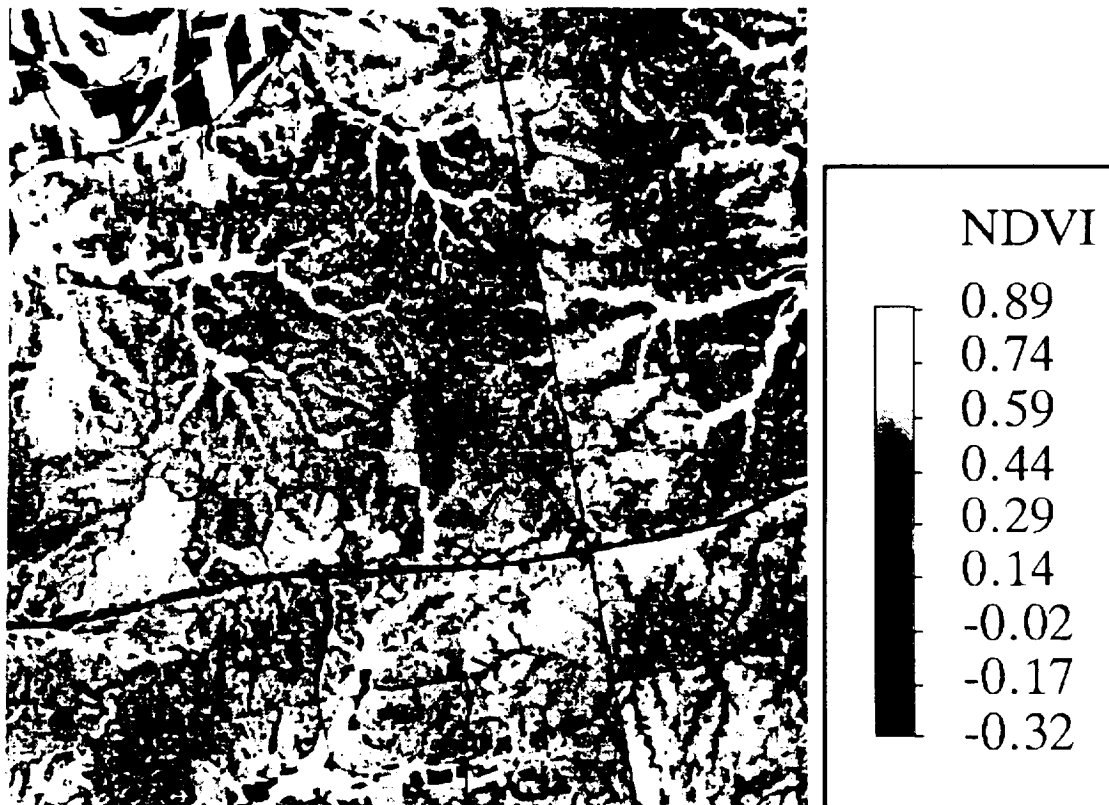


FIG. 9. Normalized vegetation index (NDVI) derived for part of the FIFE area from the 15 August 1987 overpass. Resolution is 30 m.

at the surface flux measurement stations. A principal aim of the procedure is to extend the observations of sensible and latent heat fluxes spatially from the surface flux stations by combining the TM satellite thermal data with the station data. A TM-derived estimate of surface temperature was estimated for the locations within the FIFE area, corresponding to the different surface flux stations. In the 15 km \times 15 km FIFE area, there were 19 flux stations that were used in this analysis (see Sellers et al. 1989; Hall et al. 1992). The TM surface temperature estimates and the station sensible heat measurements can be combined to provide a transfer coefficient of the following form for the TM data:

$$g_{st} = \frac{H_{st}}{\rho C_p (T_s - T_a)}, \quad (5)$$

where ρ is air density (1.19 kg m^{-3}), C_p is specific heat for air at constant pressure (at 25°C , 1005 J kg K^{-1}), H_{st} is the observed station sensible heat, T_a is the observed station air temperature, and T_s the TM-derived surface temperature. Equation (5) is constructed so that g_{st} is equivalent to the inverse of the aerodynamic resistance term, assuming that all the variables on the right-hand side of (5) are measured accurately. The variable g_{st} can be interpreted as an "effective" coef-

ficient that represents not only the aerodynamic resistance but also the effect of errors in T_s and measurement errors in H_{st} . The latter two may be quite large (Smith et al. 1992; Hall et al. 1992). In the analysis by Hall et al. (1992), they found that the TM-derived surface temperatures are high by about 3°C , which is sufficient to result in large errors in computed sensible heat fluxes.

The 19 g_{st} factors were interpolated across the 15 km \times 15 km FIFE area through geostatistical kriging. Similarly, T_a was also interpolated across the site. Using this field and the TM-derived surface temperature (both at a 120-m resolution), the sensible heat flux can be estimated over the domain by inverting (5). This allowed the estimation of the sensible heat across the FIFE area in a manner that is consistent with surface flux station observations. This field is referred to herein as H_d .

The TM-derived latent heat flux was estimated assuming that the sum of the averaged latent and sensible heat fluxes for the station data and the TM-derived fluxes would be equal.

While the above procedure could be refined, the resulting spatial patterns of sensible and latent heat fluxes appear to reflect quite accurately the underlying features within the FIFE area. Figures 12 and 13 give the



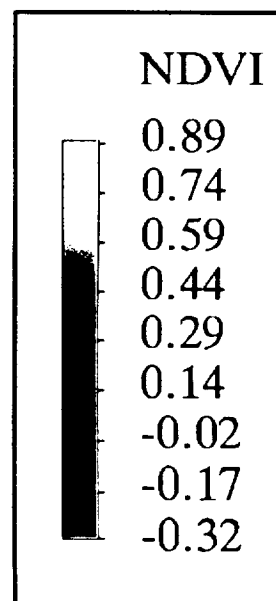
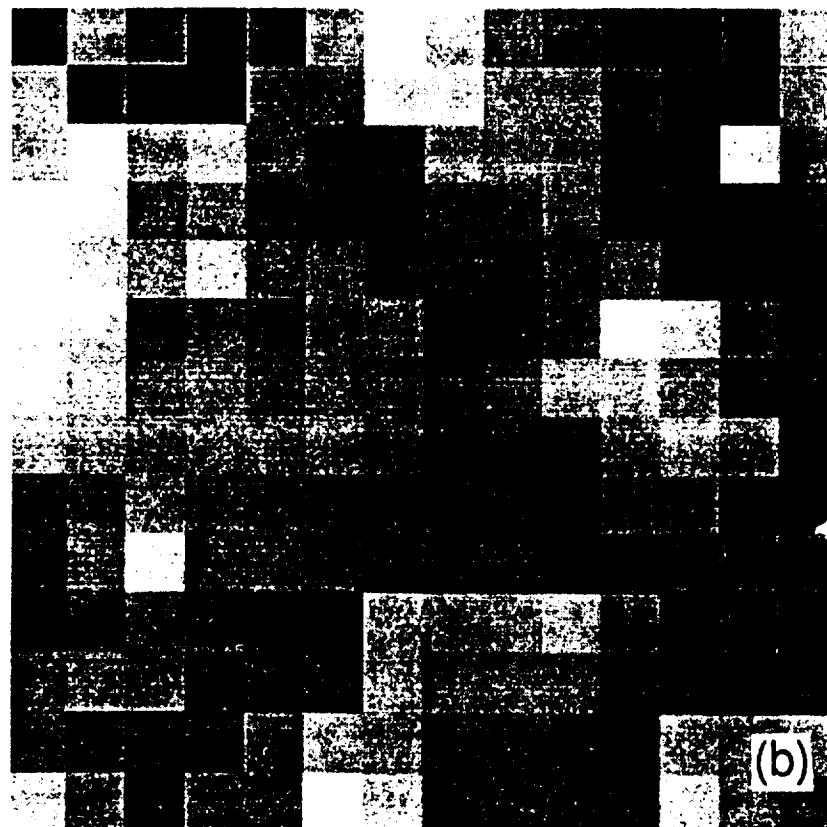
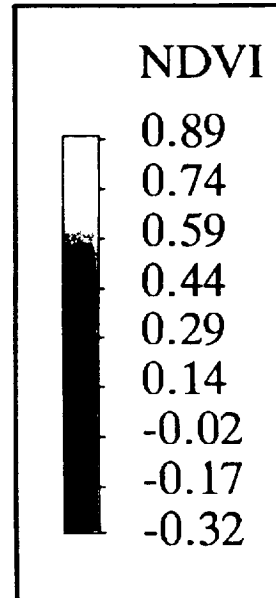


FIG. 10. Aggregated normalized vegetation index (NDVI) for part of the FIFE area for 15 August 1987. The images were derived using data from Fig. 9. Levels of aggregation into each are (a) 300 m \times 300 m, (b) 750 m \times 750 m, and (c) 1500 m \times 1500 m.



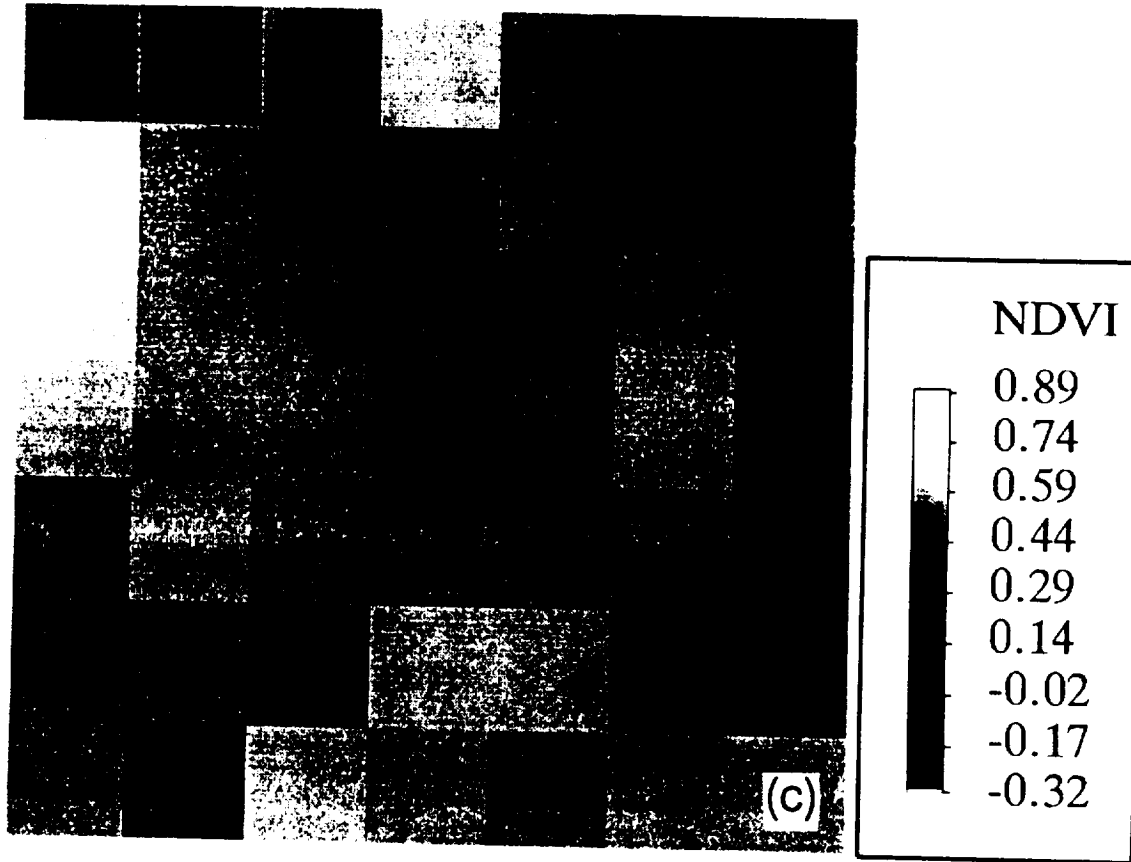


FIG. 10. (Continued)

derived images. Notice that the heavy vegetation in the southwest portion of the area (lower left) show up as having low sensible heat and high latent heat fluxes, as one would expect. Also, the interstate highway that crosses the area (east-west) can also be seen quite clearly. Some effect of the kriging can be seen as striping within the image.

The estimates in Figs. 12 and 13 are based on the TM surface radiances at a 120-m resolution. The images were also calculated using radiances that were first aggregated five times (into $600 \text{ m} \times 600 \text{ m}$ pixels) and aggregated 25 times (into $3000 \text{ m} \times 3000 \text{ m}$ pixels). Using these aggregated resolutions, the sensible and latent heat fluxes were calculated over the FIFE area in the same manner as for the 120-m data. Figures 14 and 15 present the aggregated images for sensible and latent heat fluxes.

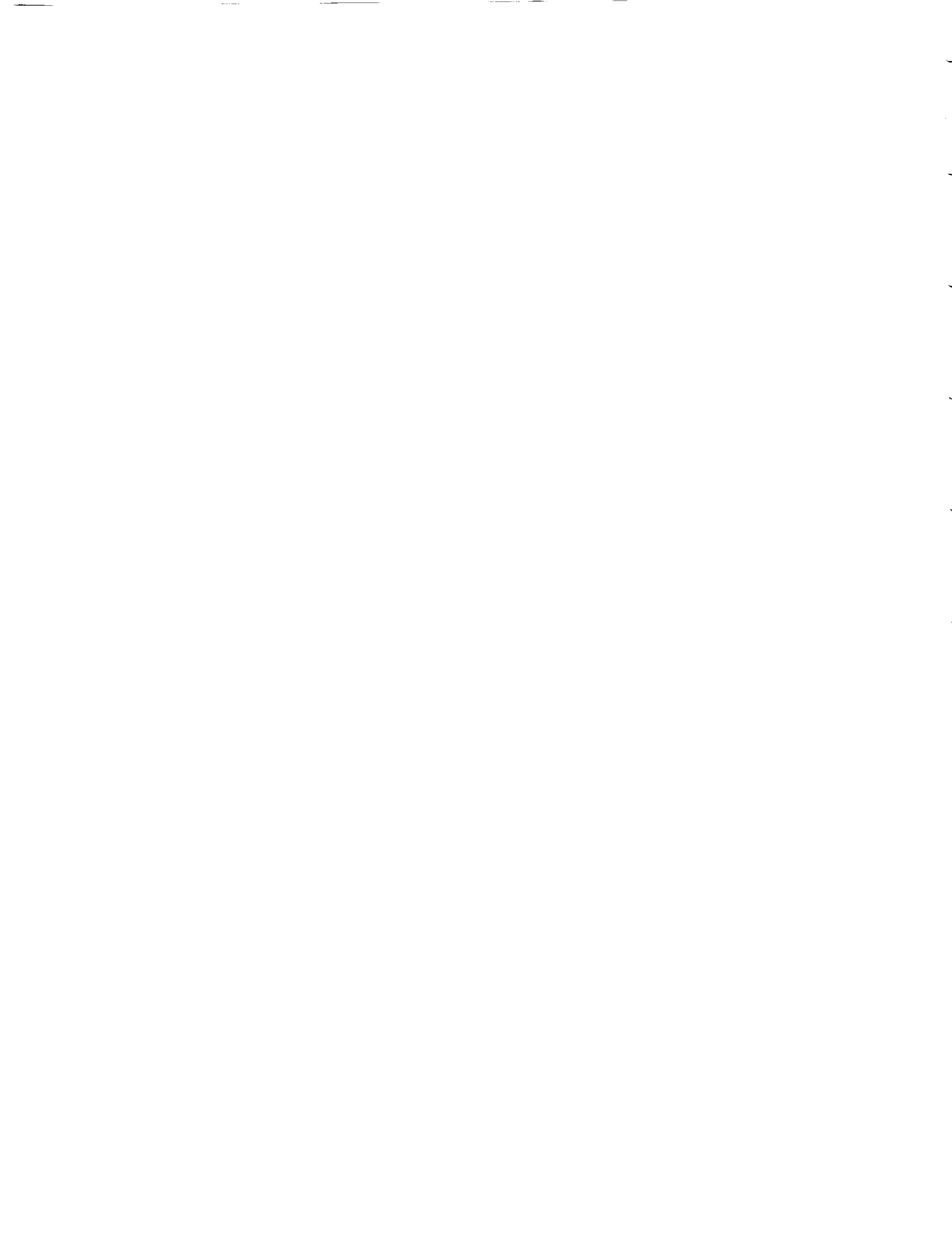
Scatter plots comparing the aggregated fluxes (using the 120-m thermal data) and the derived fluxes, based on aggregated radiances, are presented in Figs. 16 and 17 for the case when the level of aggregation was 25 times. These figures show that the scaling of thermal radiances prior to estimating scaled sensible and latent heat fluxes results in the same derived fluxes as obtained from scaling up small-scale derived fluxes; that is, the scaling of sensible and latent heat fluxes is linear, at

least for the 15 August 1987 FIFE TM data. Figures 18 and 19 show the variability across FIFE, with different levels of aggregation for sensible and latent heat fluxes. Also shown are the means derived from the detailed image (solid line) but based on the aggregated image (dashed line). For both images (and especially the latent heat fluxes shown in Fig. 19), it is essentially impossible to differentiate these two means, indicating that the scaling is linear.

5. Results and discussion

The purpose of this paper is to review recent results for the scaling of water and energy fluxes from the land component of the climate system. Three sets of experiments were presented. The first was the hydrologic response at the scale of a catchment (but could easily be at a GCM grid scale), in which spatial variability in topography, soils, and hydrologic inputs (rainfall, in this case) resulted in spatially variable responses.

The second experiment was the application of SiB to a spatially heterogeneous domain based on data from Amazonia. Here, the experiments studied the impacts of variability in vegetation density (through the leaf-area index), initial soil wetness, and rainfall (both spa-



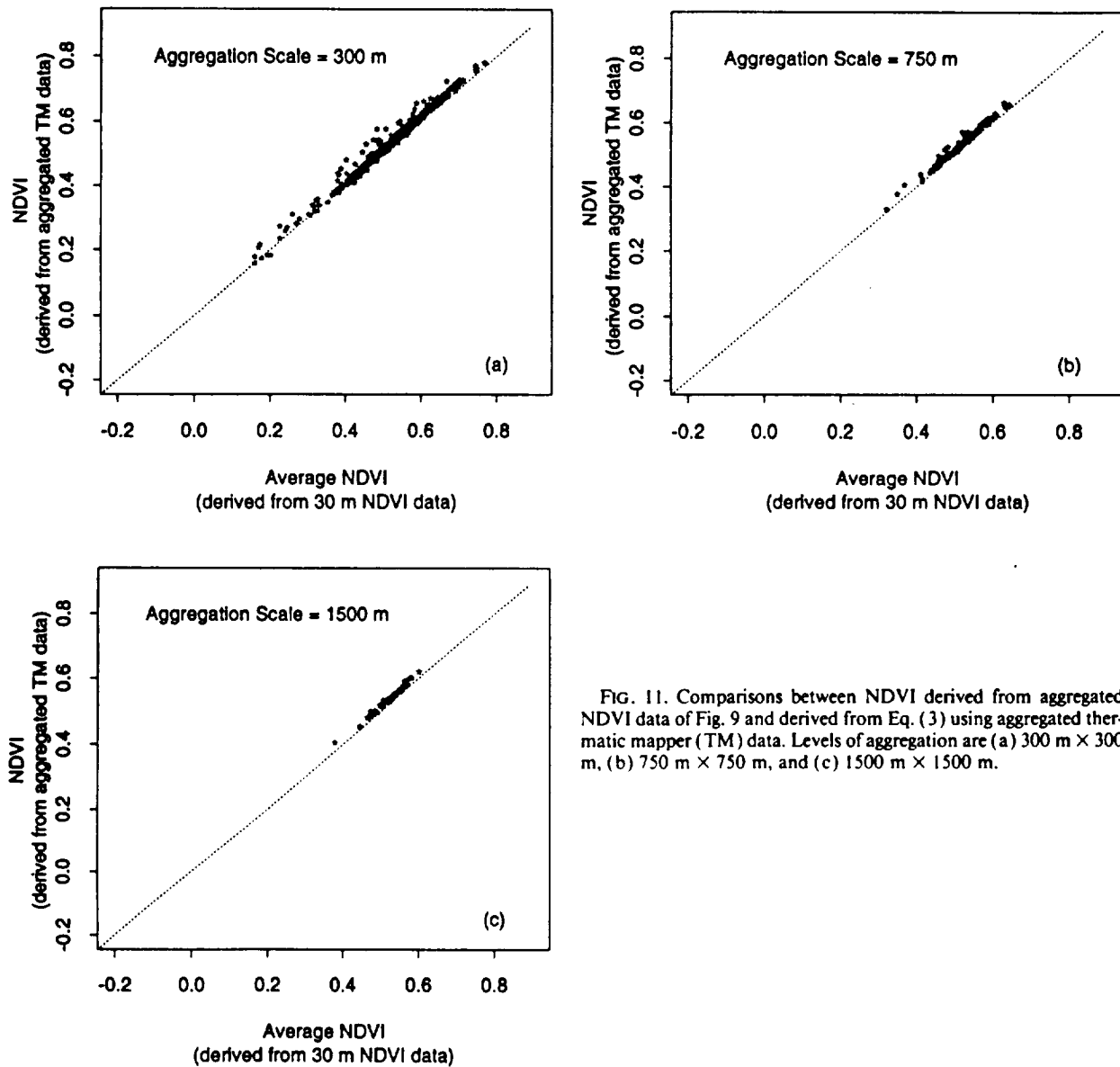


FIG. 11. Comparisons between NDVI derived from aggregated NDVI data of Fig. 9 and derived from Eq. (3) using aggregated thematic mapper (TM) data. Levels of aggregation are (a) $300 \text{ m} \times 300 \text{ m}$, (b) $750 \text{ m} \times 750 \text{ m}$, and (c) $1500 \text{ m} \times 1500 \text{ m}$.

tially and temporally) on the derived latent heat flux over a 43-day observation period.

The third set of experiments studied the scaling in the normalized vegetation index (NDVI) and sensible and latent heat fluxes as derived from a thematic mapper (TM) overpass of the FIFE area on 15 August 1987. Variations in surface conditions due to vegetation characteristics, as well as topography and soils, lead to significant variations in the TM-derived variables, as is shown in the presented images.

The major result from the three sets of experiments is that the scaled fields are equivalent to the fields derived from scaled inputs and parameters. The implication of this result is that the fluxes and land characteristics essentially scale linearly. More importantly,

these results appear to suggest that "equivalent" parameters can be used in scaled models (or macroscale models) for the calculation of spatially averaged quantities as long as the equivalent parameters reflect the statistical characteristics of the subscale variability. The one exception to this result was the temporal averaging of rainfall in the SiB experiment. In this case, the temporally averaged latent heat fluxes were significantly different from the latent heat fluxes derived from the temporally averaged rainfall. This implies that the latent heat scales nonlinearly with respect to the rainfall rates.

These results must be balanced with the knowledge that the experiments presented were neither exhaustive nor complete. The modeling results with SiB did not



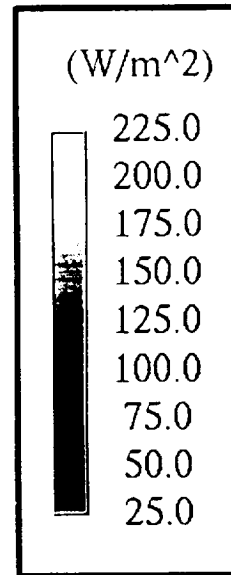


FIG. 12. Sensible heat flux for the FIFE area. The data are averaged over 15 August 1987 and are derived from the thermatic mapper (TM) overpass. Resolution is 120 m.

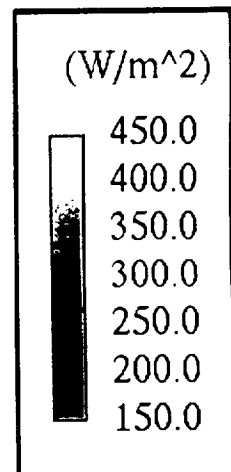


FIG. 13. Latent heat flux for the FIFE area. The data are averaged over 15 August 1987 and are derived from the thermatic mapper (TM) overpass. Resolution is 120 m.



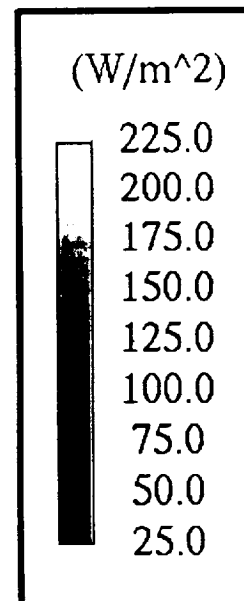
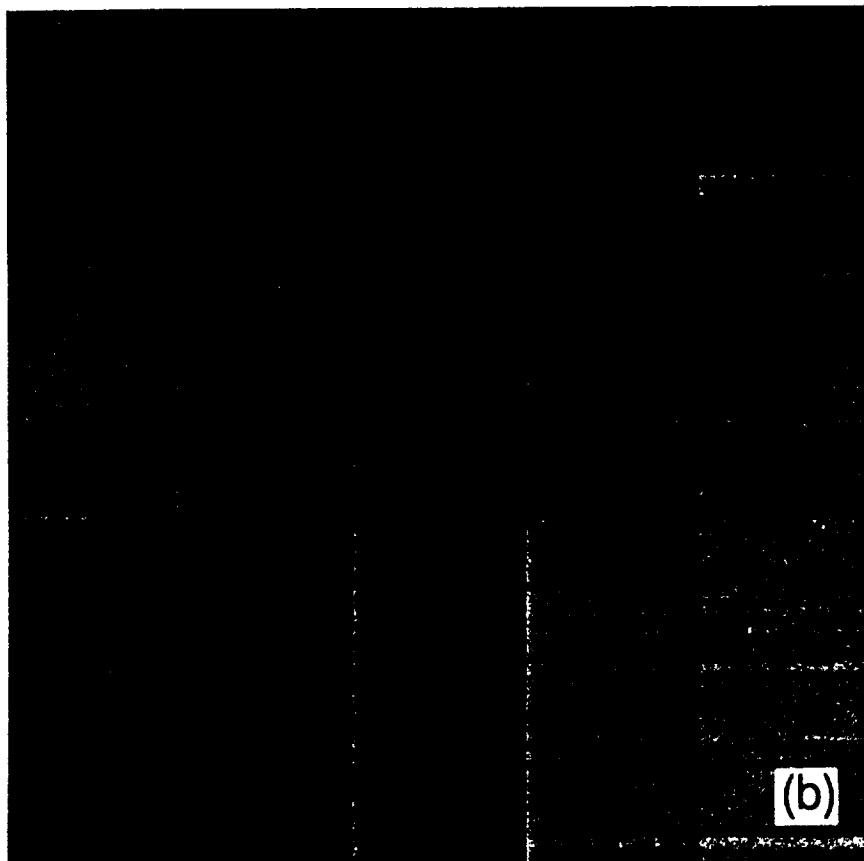
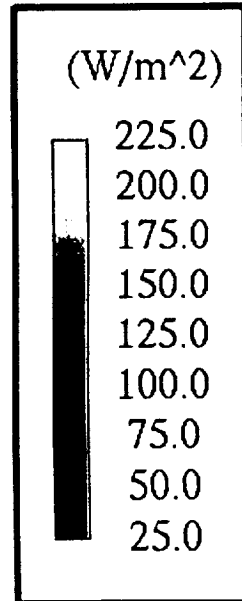
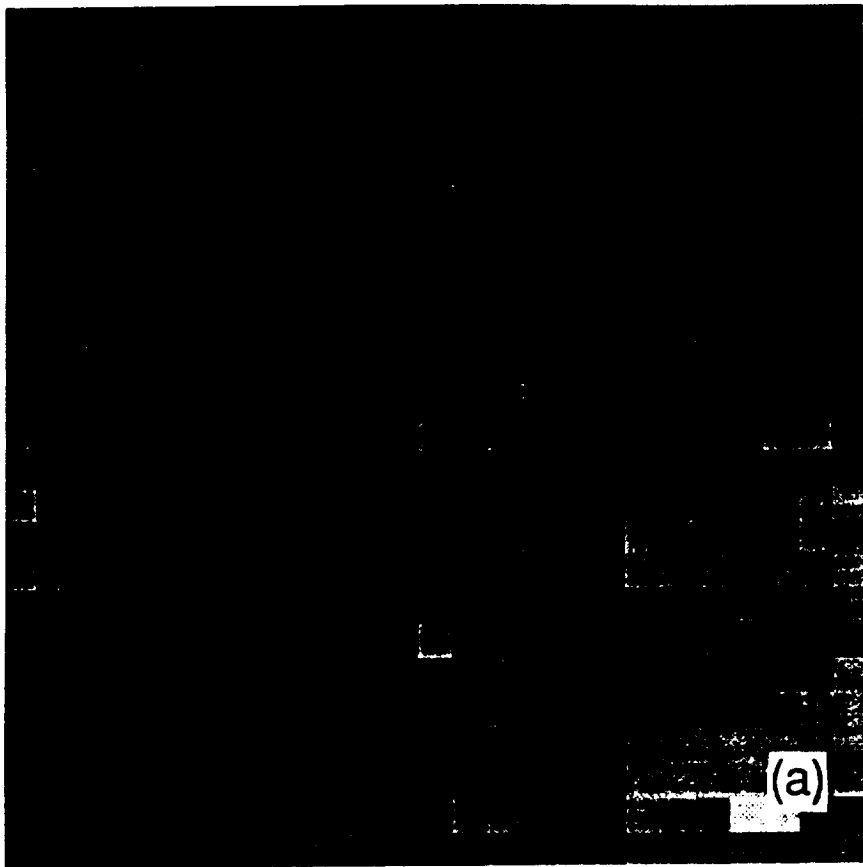


FIG. 14. Aggregated sensible heat flux for the FIFE area using data from Fig. 12. Levels of aggregation are (a) 600 m x 600 m and (b) 3000 m x 3000 m.

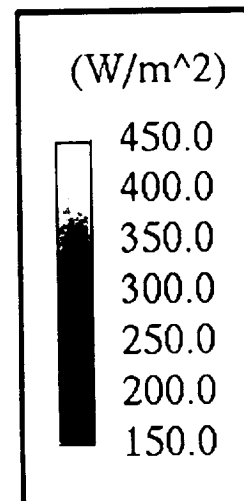
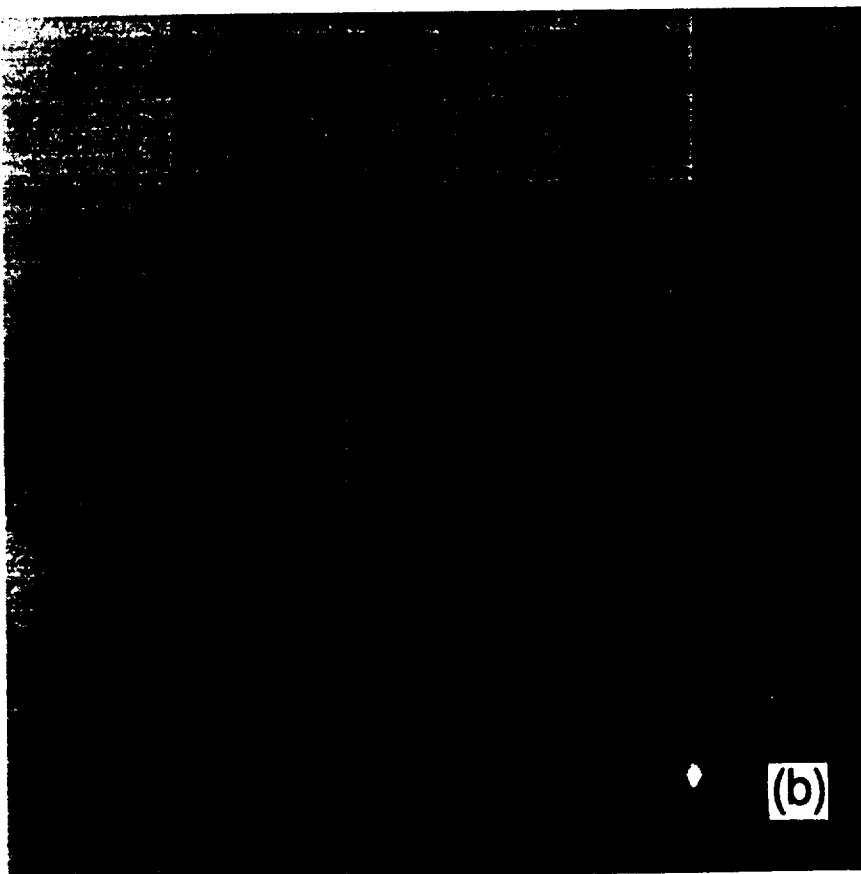
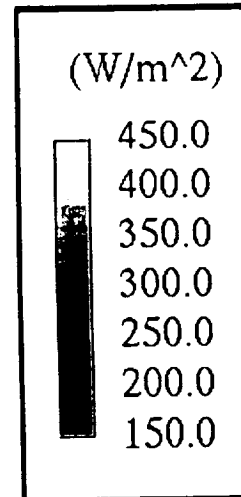
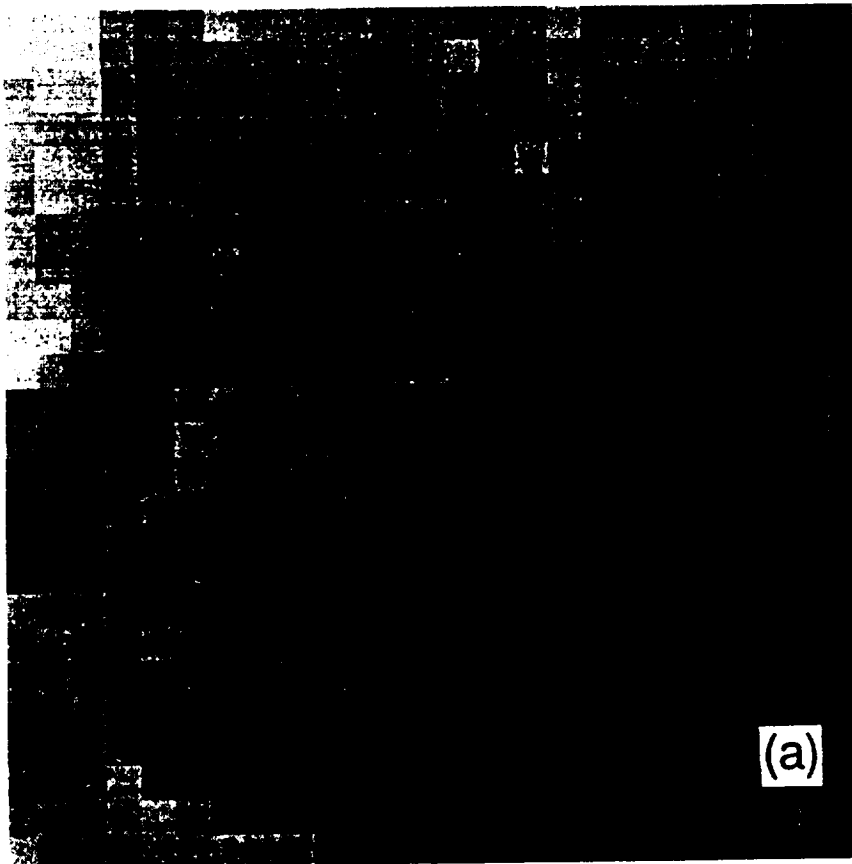
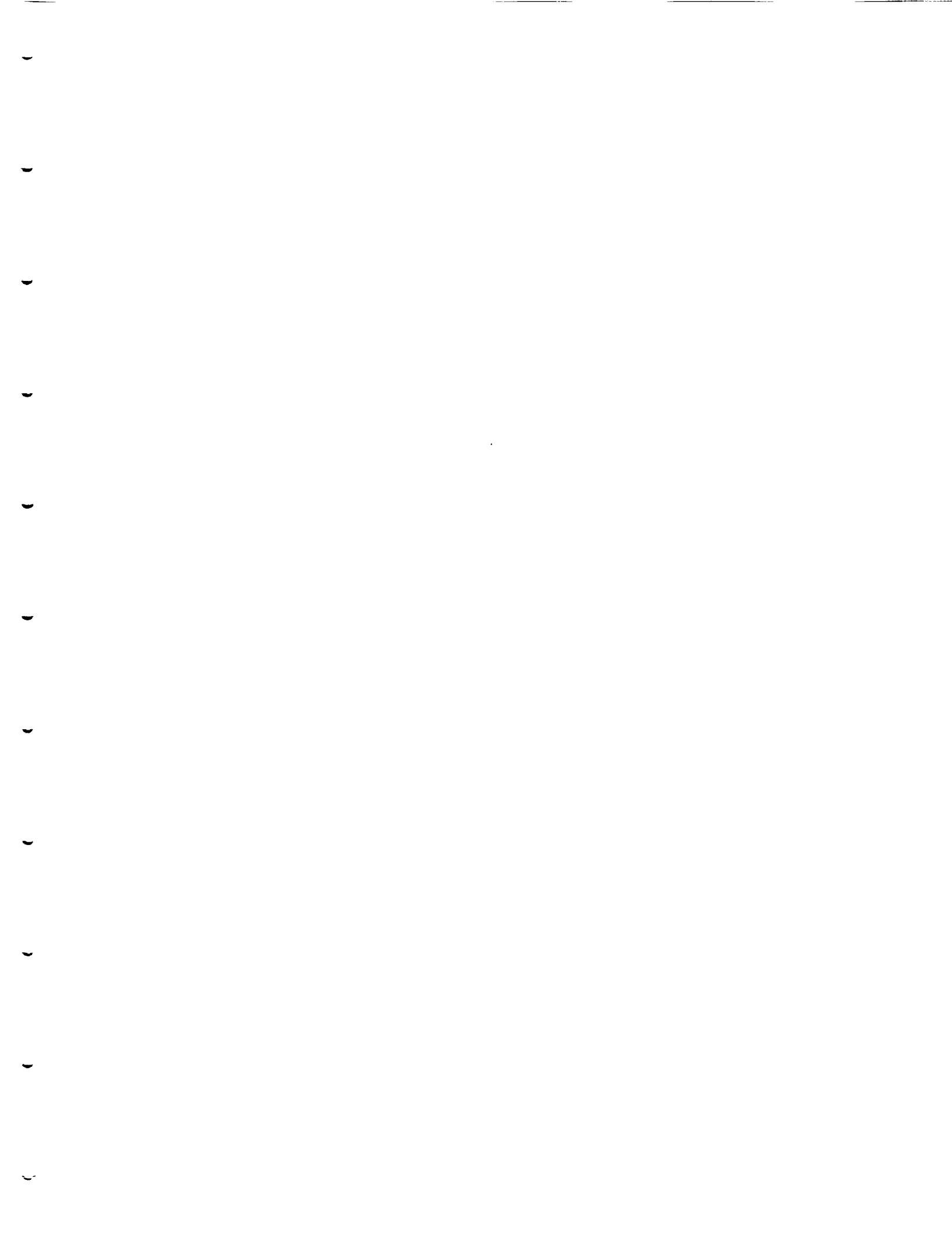


FIG. 15. Aggregated latent heat flux for the FIFE area using the data from Fig. 13. Levels of aggregation are (a) 600 m x 600 m and (b) 3000 m x 3000 m.



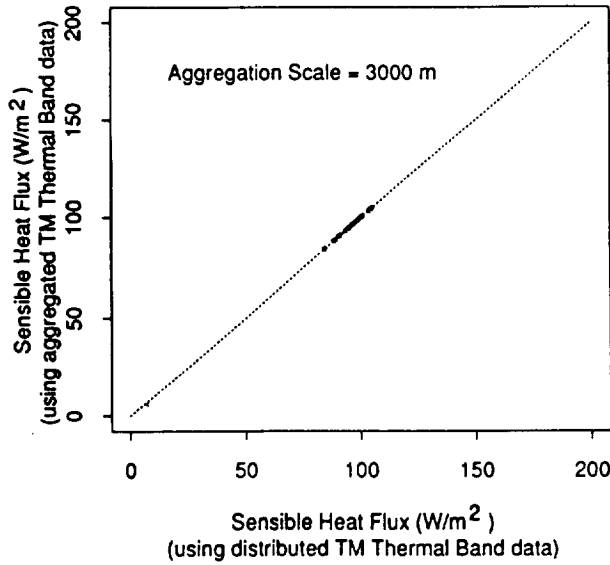


FIG. 16. Comparisons between sensible heat flux derived from aggregated sensible heat flux data of Fig. 12 and derived from aggregated thermatic mapper (TM) thermal-band radiances at an aggregation level of $3000\text{ m} \times 3000\text{ m}$.

include an interactive boundary layer whose effects can lead to nonlinearities under specific heterogeneities (Avisar and Pielke 1989). The satellite experiments represented a particular condition in which the range of temperatures was reasonably small, resulting in effectively linear models that transfer radiances to fluxes. Whether such ranges are typical of natural systems is

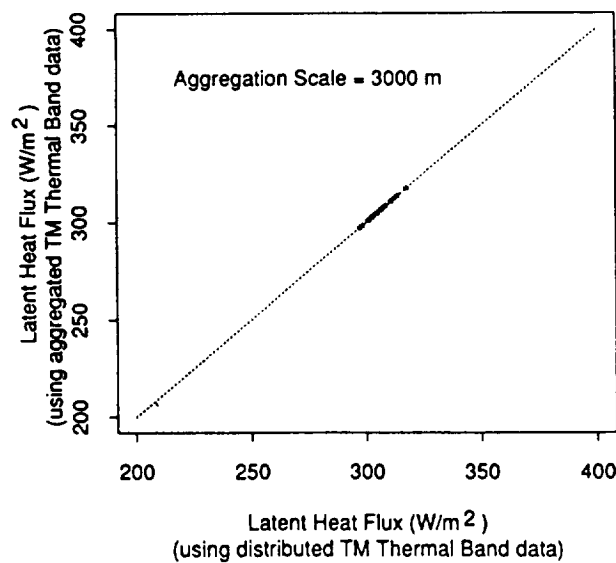


FIG. 17. Comparisons between latent heat flux derived from aggregated latent heat flux data of Fig. 13 and derived from aggregated thermatic mapper (TM) thermal-band radiances at an aggregation level of $3000\text{ m} \times 3000\text{ m}$.

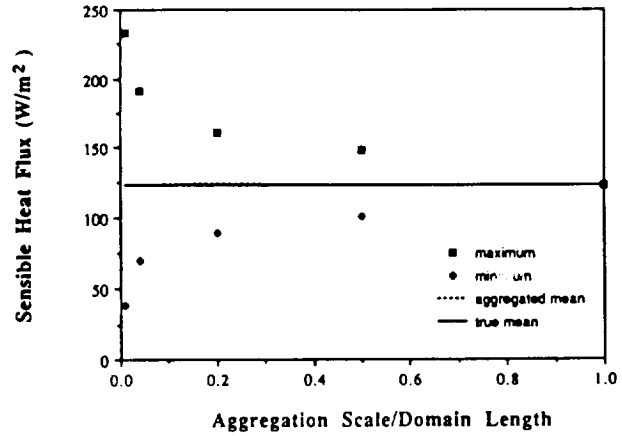


FIG. 18. Effect of aggregation on the variability of sensible heat across the FIFE domain for the 15 August 1987 TM overpass.

unknown until a greater number of analyses are done.

In the Introduction it was suggested that there were two current thoughts concerning subgrid variability: (i) that subgrid processes have a significant, nonlinear effect on large-scale processes that prevents simple scaling, and (ii) effective parameters within an appropriate macroscale model can represent large climatic fluxes. This basic scaling question is still unresolved, but hopefully the work presented here has provided some insight into these issues.

In the hydrologic-response experiment, the concept of the representative elementary area (REA) (Wood et al. 1988) was used to find the scale in which the macroscale model is a valid model for the scaled process. The results of the experiments carried out here suggest that the REA concept has wide applicability for a range of climate problems, and that it appears that the REA will be on the order of a few (1.5 to 3)

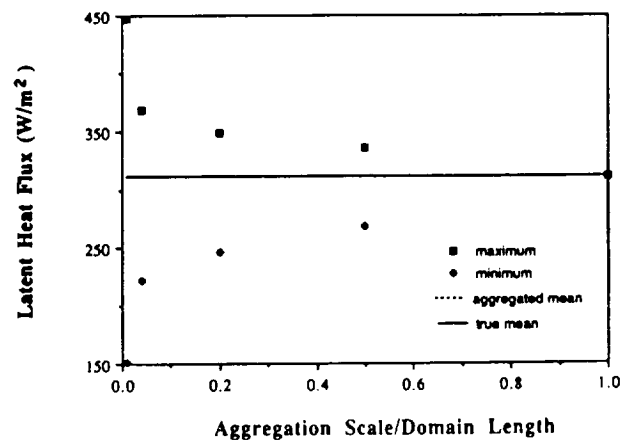


FIG. 19. Effect of aggregation on the variability of latent heat across the FIFE domain for the 15 August 1987 TM overpass.



correlation lengths of the dominant heterogeneity. At scales larger than the REA scale, there has been enough "sampling" of the heterogeneities that the average response is well represented by a macroscale model with average parameters.

It is hoped that the experiments presented in this paper motivate related research, possibly with more complex land-atmospheric models or through a wider range of satellite data, that can help resolve the basic issue concerning scaling in natural systems. What must be determined are the scaling properties for reasonably sized domains in natural systems, where the range of variability (in vegetation, rainfall, radiance, topography, soils, etc.) is reflective of these natural systems. The results in this paper provide one perspective.

Acknowledgments. The research presented here was supported in part by the National Aeronautics and Space Administration (NASA) through Grants NAGW-1392 and NAG-899; this support is gratefully acknowledged. The authors also wish to thank Jay Famiglietti who helped develop the water-balance model for Kings Creek and Dom Thongs for helping with running the model and with the graphics.

REFERENCES

- Abramopoulos, F., C. Rosenzweig, and B. Choudhury, 1988: Improved ground hydrology calculations for global climate models (GCMs): Soil water movement and evapotranspiration. *J. Climate*, **1**, 921-941.
- Avissar, R., and R. A. Pielke, 1989: A parameterization of heterogeneous land surface for atmospheric numerical models and its impact on regional meteorology. *Mon. Wea. Rev.*, **117**, 2113-2136.
- Beven, K. J., 1986a: Runoff production and flood frequency in catchments of order n : An alternative approach. *Scale Problems in Hydrology*, V. K. Gupta, I. Rodriguez-Iturbe, and E. F. Wood, Eds., D. Reidel, 107-131.
- , 1986b: Hillslope runoff processes and flood frequency characteristics. *Hillslope Processes*, A. D. Abrahams, Ed., George Allen and Unwin, 187-202.
- , and M. J. Kirkby, 1979: A physically based variable-contributing area model of basin hydrology. *Hydrol. Sci. Bull.*, **24**, 43-69.
- Budyko, M. I., 1956: *Heat balance of the earth's surface*. U.S. Weather Bureau, Washington, DC.
- Charney, J., W. Quirk, S. Chow, and J. Kornfeld, 1977: A comparative study of the effects of albedo change on drought in semiarid regions. *J. Atmos. Sci.*, **34**, 1366-1385.
- Dickinson, R. E., 1984: Modeling evapotranspiration for three dimensional global climate models: climate processes and climate sensitivity. *Geophys. Monogr.*, **29**, Maurice Ewing Volume 5, Amer. Geophys. Union, Washington, DC, 58-72.
- , A. Henderson-Sellers, P. J. Kennedy, and M. F. Wilson, 1986: Biosphere-atmosphere transfer scheme (BATS) for the NCAR community climate model. NCAR Technical Note, 69 pp.
- Entekhabi, D., and P. S. Eagleson, 1989: Land surface hydrology parameterization for atmospheric general circulation models including subgrid scale spatial variability. *J. Climate*, **2**, 816-831.
- Famiglietti, J., and E. F. Wood, 1991a: Evapotranspiration and runoff from large land areas: Land surface hydrology for atmospheric general circulation models. *Land Surface-Atmospheric Interactions for Climate Models: Observations, Models, and Analyses*, Eric F. Wood, Ed., Kluwer, 179-204.
- , and —, 1991b: Comparison of passive microwave and model-derived estimates for soil moisture fields. *Proc. Fifth International Colloquium—Physical Measurements and Signatures in Remote Sensing*, Courchevel, France, European Space Agency, 321-326.
- , E. F. Wood, M. Sivapalan, and D. J. Thongs, 1992: A catchment scale water balance model for FIFE. *J. Geophys. Res.*, **97**(D17), 18 997-19 007.
- Hall, F. G., K. F. Huemmrich, S. J. Goetz, P. J. Sellers, J. E. Nickeson, 1992: Satellite Remote Sensing of Surface Energy Balance: Success, Failures and Unresolved Issues in FIFE. *J. Geophys. Res.*, in press.
- Holwill, C. J., and J. B. Stewart, 1992: Spatial variability of evaporation derived from aircraft and groundbased data. *J. Geophys. Res.*, **97**(D17), 18 673-18 680.
- Markham, B. L., and J. L. Barker, 1986: Landsat MSS & TM post-calibration dynamic ranges, exoatmospheric reflectances and at satellite temperatures. *EOSAT Landsat Tech. Note*, **1**, 3-8.
- Rowntree, P. R., and J. R. Bolton, 1983: Simulation of the atmospheric response to soil moisture anomalies over Europe. *Quart. J. Roy. Meteor. Soc.*, **109**, 501-526.
- Sato, N., P. J. Sellers, D. A. Randall, E. K. Schneider, J. Shukla, J. L. Kinter III, Y-T Hou, and E. Albertazzi, 1989: Effects of implementing the simple biosphere model in a general circulation model. *J. Atmos. Sci.*, **46**, 2757-2782.
- Sellers, P. J., and J. L. Dorman, 1987: Testing the simple biosphere model (SiB) using point micrometeorological and biophysical data. *J. Climate Appl. Meteor.*, **26**, 622-651.
- , Y. Mintz, Y. C. Sud, and A. Dalcher, 1986: A simple biosphere model (SiB) for use within general circulation models. *J. Atmos. Sci.*, **43**, 1986.
- , F. G. Hall, G. Asrar, D. E. Strebel, and R. E. Murphy, 1988: The First ISLSCP Field Experiment (FIFE). *Bull. Amer. Meteor. Soc.*, **69**, 22-27.
- , W. J. Shuttleworth, J. L. Dorman, A. Dalcher, and J. M. Roberts, 1989: Calibrating the simple biosphere model for amazonian tropical forest using field and remote sensing data. Part I: Average calibration with field data. *J. Appl. Meteor.*, **28**, 727-759.
- Shukla, J., and Y. Mintz, 1982: The influence of land-surface evapotranspiration on earth's climate. *Science*, **215**, 1498-1501.
- , C. Nobre, and P. J. Sellers, 1990: Amazon deforestation and climate change. *Science*, **247**, 1322-1325.
- Sivapalan, M., K. J. Beven, and E. F. Wood, 1987: On hydrological similarity. II: A scaled model of storm runoff production. *Water Resour. Res.*, **23**, 2266-2278.
- Smith, E. A., A. Y. Hsu, W. L. Crosson, R. T. Field, L. J. Fritschen, R. J. Gurney, E. T. Kanemasu, W. Kustas, D. Nie, W. J. Shuttleworth, J. B. Stewart, S. B. Verma, H. Weaver, and M. Wesley, 1992: Area averaged fluxes and their time-space variability over the FIFE Experimental Domain. *J. Geophys. Res.*, **97**(D17), 18 599-18 622.
- Sud, Y. C., P. Sellers, M. D. Chow, G. W. Walker, and W. E. Smith, 1990: Influence of biosphere on the global circulation and hydrologic cycle—A GCM simulation experiment. *Agric. For. Meteorol.*, **52**, 133-188.
- Walker, J. M., and P. R. Rowntree, 1977: The effect of soil moisture on circulation and rainfall in a tropical model. *Quart. J. Roy. Meteor. Soc.*, **103**, 29-46.
- Wood, E. F., 1991: Global scale hydrology: Advances in land surface modeling. *Rev. Geophys.*, **Suppl.**, **29**, 193-201.
- , M. Sivapalan, K. J. Beven, and L. Band, 1988: Effects of spatial variability and scale with implications to hydrologic modeling. *J. Hydrol.*, **102**, 29-47.
- , —, —, 1990: Similarity and scale in catchment storm response. *Rev. Geophys.*, **28**, 1-18.



